







RESEARCH ARTICLE

10.1029/2023MS003655

Improving Phenology Representation of Deciduous Forests in the Community Land Model: Evaluation and Modification Using Long-Term Observations in China

Yan Lv^{1,2,3}, Li Zhang^{1,2,4} , Pan Li⁵, Honglin He^{1,2,4} , Xiaoli Ren^{1,2,4}, Zongqiang Xie⁶ , Yang Wang⁶, Anzhi Wang⁷, FuSun Shi⁸, Ruiying Chang⁹ , Jingfeng Xiao¹⁰ , and Xufeng Wang¹¹ 

Key Points:

- The involvement of chill accumulation with heat requirement in leaf unfolding models can improve the model performance
- We propose a new leaf falling model by considering the relationship between summer temperature and aging state threshold, which improves the model performance
- The revise of deciduous phenological model in CLM4.5 improves the simulation of gross primary productivity by influencing carbon uptake duration and amplitude

Supporting Information:

Supporting Information may be found in the online version of this article.

Correspondence to:

L. Zhang and H. He,
li.zhang@igsnr.ac.cn;
hehl@igsnr.ac.cn

Citation:

Lv, Y., Zhang, L., Li, P., He, H., Ren, X., Xie, Z., et al. (2023). Improving phenology representation of deciduous forests in the Community Land Model: Evaluation and modification using long-term observations in China. *Journal of Advances in Modeling Earth Systems*, 15, e2023MS003655. <https://doi.org/10.1029/2023MS003655>

Received 7 FEB 2023

Accepted 29 SEP 2023

Author Contributions:

Funding acquisition: Li Zhang

Methodology: Yan Lv

Supervision: Li Zhang

Validation: Yan Lv

Writing – original draft: Yan Lv

¹Key Laboratory of Ecosystem Network Observation and Modeling, Institute of Geographic Sciences and Natural Resources Research, Chinese Academy of Sciences, Beijing, China, ²National Ecosystem Science Data Center, Institute of Geographic Sciences and Natural Resources Research, Chinese Academy of Sciences, Beijing, China, ³University of Chinese Academy of Sciences, Beijing, China, ⁴College of Resources and Environment, University of Chinese Academy of Sciences, Beijing, China, ⁵School of Earth System Science, Tianjin University, Tianjin, China, ⁶Institute of Botany, Chinese Academy of Sciences, Beijing, China, ⁷Institute of Applied Ecology, Chinese Academy of Sciences, Shenyang, China, ⁸Chengdu Institute of Biology, Chinese Academy of Sciences, Chengdu, China, ⁹Institute of Mountain Hazards and Environment, Chinese Academy of Sciences, Chengdu, China, ¹⁰Earth Systems Research Center, Institute for the Study of Earth, Oceans, and Space, University of New Hampshire, Durham, NH, USA, ¹¹Key Laboratory of Remote Sensing of Gansu Province, Heihe Remote Sensing Experimental Research Station, Northwest Institute of Eco-Environment and Resources, Chinese Academy of Sciences, Lanzhou, China

Abstract Phenology is an important factor indicating environmental changes and regulates the variations of carbon, water, and energy exchange. However, phenology models exhibit large uncertainties due to limited understanding of its mechanisms. In this study, we modified deciduous phenology scheme based on the evaluation of different phenological models using long-term observations at Chinese Ecosystem Research Network with CLM4.5. The alternating leaf unfolding model and summer-influenced autumn leaf falling model that we proposed, performed best in simulating leaf-unfolding and leaf-falling. Compared with the observed and remote-sensed phenology, the modified model could better simulate the phenological dates at the site and regional scale. Moreover, the modified model improved the simulation of gross primary productivity (GPP) by decreasing the errors of modeled carbon uptake duration and amplitude. Furthermore, the advance in leaf-unfolding slowed down from 0.20 days/year during 1981–2015 to 0.11 days/year during 2016–2100 under RCP4.5 because of the slowdown of climate warming, but the delay in leaf-falling changed little. By the last decade of the twenty-first century, the leaf-unfolding would advance (8 days) and leaf-falling would delay (16 days). The subtropical region had large interannual variation (IAV) in leaf-unfolding because of the high sensitivity to temperature. The phenological dates IAV in the cold temperate region increased due to enhanced temperature IAV. We suggest that the deciduous phenology models, especially the leaf-falling process, used in Community Land Model need to be improved to reduce the errors in predicting phenology and carbon flux in the future.

Plain Language Summary As an important factor indicating climate and environmental changes, phenology plays an important role in regulating the variation of carbon, water, and energy exchange. Due to limited understanding of phenology mechanisms, the simulation of phenology remains large uncertainties. In this study, we evaluated and modified the leaf unfolding and leaf falling models using the long-term phenological observations with the Community Land Model (CLM4.5), validated the modified leaf-unfolding and leaf-falling models by observed phenology and remote-sensing phenology data, examined the ability of CLM4.5 with modified deciduous phenology submodels in simulating gross primary productivity, and used the modified phenology models to predict the changes in phenological dates in the future. Our results suggest that the deciduous phenology models, especially the leaf-falling process, used in the CLM is urgent to be improved to reduce the errors in predicting growing season length and carbon fluxes in deciduous forests in the context of climate change.

© 2023 The Authors. Journal of Advances in Modeling Earth Systems published by Wiley Periodicals LLC on behalf of American Geophysical Union. This is an open access article under the terms of the [Creative Commons Attribution-NonCommercial-NoDerivs License](https://creativecommons.org/licenses/by/4.0/), which permits use and distribution in any medium, provided the original work is properly cited, the use is non-commercial and no modifications or adaptations are made.

Writing – review & editing: Yan Lv, Li Zhang, Pan Li, Honglin He, Xiaoli Ren, Zongqiang Xie, Yang Wang, Anzhi Wang, FuSun Shi, Ruiying Chang, Jingfeng Xiao

1. Introduction

Phenology plays an important role in regulating the ecosystem carbon uptake process (Abu-Asab et al., 2001; Bradley et al., 1999). Vegetation phenology, for example, leaf unfolding and falling, regulates many ecosystem processes, such as the carbon cycle, water evaporation, mineralization, and absorption of nutrients (Estiarte and Peñuelas, 2015; Piao et al., 2007). Especially prolonged growing season length due to earlier leaf unfolding dates and later leaf falling dates could increase the carbon assimilation time and result in accumulation of more organic matter (Richardson et al., 2009). Deciduous and mixed forests contain 30% of the forest ecosystems globally, which are one of the main contribution areas to the temporal variation of land carbon sink in Northern America (Shiga et al., 2018) and the globe (Huang and Xia, 2019). Nevertheless, the poor representation of deciduous phenology in current terrestrial biosphere models hinder their ability to simulate the carbon fluxes and responses to climate change in deciduous forests (Richardson et al., 2012). Therefore, accurate estimation of both leaf unfolding and leaf falling dates is of great importance in predicting the exchanges of carbon dioxide between deciduous ecosystems and the atmosphere and understanding the response of deciduous ecosystems to climate change (Churkina et al., 2005; Z. Fu et al., 2017; Piao et al., 2007).

The phenological model is a feasible and effective method for assessing relationships between phenology and climate and predicting phenological changes under varied climatic and anthropogenic scenarios (B. Li et al., 2015; Zhao et al., 2013). Underlying mechanistic processes governing phenological events are empirically represented via statistical relationships in the phenological model (Piao et al., 2019). The growth and dormant periods comprise the annual cycle of woody plants (Hänninen, 1996). Scholars indicated that the heat requirement could break the dormancy (Murray et al., 1989). This method has been widely used to predict the leaf unfolding dates in most terrestrial biosphere models, such as BIOME-BGC (White et al., 1997), CARAB (Horemans et al., 2017), CLASS 2.7 (Verseghy et al., 1993), Community Land Model (CLM) 4.5 (Oleson et al., 2013), DLEM (Tian et al., 2011), IBIS (Foley et al., 1996), LPJ-DGVM (Sitch et al., 2003), and ISAM (El Masri et al., 2015). These models predict earlier leaf unfolding dates in colder regions but later leaf unfolding dates in warmer regions (Chen et al., 2016; Chuine et al., 2010). Furthermore, the dormancy of wood plants has been distinguished into rest and quiescence phases (Kramer, 1994). Rest (i.e., endodormancy) means the growth-arresting conditions prevent the growth, even when external conditions are normally favorable. The growth-arresting conditions can be removed by chill accumulation for a prolonged period (Kramer et al., 2000). Quiescence (i.e., ecodormancy) means only unfavorable external conditions prevent the growth. When favorable temperature conditions arise, the wood plants are ready to grow (Lundell et al., 2020). Therefore, in addition to the heat requirement, a certain amount of chilling is also needed to break dormancy (Sarvas, 1972). Based on the different relationship of rest and quiescence, there are three commonly-used types of two-phase models in simulating leaf unfolding dates, that is, the sequential model, parallel model, and alternating model (Ghelardini et al., 2010; Kramer, 1994; Lechowicz, 1984). The rest and quiescence phases are assumed to be strictly separate periods in the sequential model, with no response to warm temperatures before rest release (Sarvas, 1972, 1974). In the parallel model and alternating model, rest and quiescence coexist; even when the rest has not yet been attained, a response to warm temperatures is possible (Cannell & Smith, 1983; Landsberg, 1974). The difference between the parallel model and alternating model is whether chill accumulation and heat requirement occur simultaneously or alternately. The alternating model has been used in the simulation of phenology in ecosystem models, for example, ORCHIDEE (MacBean et al., 2015) and ELM (Meng et al., 2021). Compared with long-term measurements at forest sites, these models predicted earlier start of photosynthetic uptake with biases of -28 ± 21 days (Richardson et al., 2012).

Contrary to the enormous amount of research on leaf unfolding dates, we still have little understanding of the mechanism of leaf falling dates (Chuine et al., 2010; Y. H. Fu et al., 2022; M. Wang et al., 2022). Most models predicted the dates of leaf falling based on the fixed temperature threshold (Chuine et al., 2013; Krinner et al., 2005) as in CARAIB (Horemans et al., 2017), CLASS 2.7 (Verseghy et al., 1993), DLEM (Tian et al., 2011), IBIS (Foley et al., 1996), LPJ-DGVM (Sitch et al., 2003), and ORCHIDEE (MacBean et al., 2015), the fixed daylength threshold (White et al., 1997) as in CLM4.5 (Oleson et al., 2013; Verseghy et al., 1993), and both of them (Wareing, 1956) as in BIOME-BGC (White et al., 1997), CEVSA2 (F. Gu, 2007; White et al., 1997), CTEM (White et al., 1997), and ISAM (El Masri et al., 2015). The above methods exhibited large deviations up to 15 ± 17 days in simulated end of photosynthetic uptake (Richardson et al., 2012). Delpierre et al. (2009) supposed leaf falling dates to be the result of a daylength-sensitive cold-degree day summation procedure, which has been used in the modification of phenology in the ELM model and better simulated leaf falling dates in a

boreal peatland forest (Meng et al., 2021), but cannot be applied to temperature deciduous forest areas because of the assessment at limited sites (Delpierre et al., 2009).

Numerous studies have shown overall earlier leaf unfolding dates and later leaf falling dates in most parts of the world caused by global warming (Cong et al., 2013; Liu et al., 2016; Menzel et al., 2006; Richardson et al., 2010). But there were still large discrepancies in the reported temporal autumn phenology trends in different study areas and some areas even showed opposite trends (Y. H. Fu, Campioli, et al., 2014; Jeong et al., 2012) or no significant trends (X. Wang et al., 2019). As a sensitive and significant area impacted by global climate change, China has an average temperature rise rate (0.26°C/10 year) is significantly higher than the global average level (0.15°C/10 year) in the same period (1951–2020), and phenology in China appears to have a larger change than that in Europe and North America (Ge et al., 2015). According to the predictions of future global climate, China's air temperature would increase by 0.4–2.5°C around 2100 (D. Keenan, 2014), especially in the high latitude and high-altitude regions (Yang et al., 2021). In the context of global warming, the future changes and regional differences of phenological dates and their sensitivity to climate change of deciduous forests in China are not clear.

The CLM is a state-of-the-art land surface model, which is the land component model in the Community Earth System Model (Oleson et al., 2013), and is also used in other earth system models such as CMCC-ESM2, CMCC-CM2-SR5, and NorESM-LM. The new version of CLM (CLM5) has the same seasonal deciduous phenology submodel as CLM4.5 (Lawrence et al., 2019). Thus, in this study, we aimed to improve the deciduous phenology scheme in the CLM4.5 model based on the evaluation of four leaf-unfolding models and four leaf-falling models using long-term observations at five sites of Chinese Ecosystem Research Network (CERN), and to investigate the temporal change and regional divergence in phenological dates of China's deciduous forests in the future. The four leaf-unfolding models included the spring warming model, parallel model, sequential model, and the alternating model. The four leaf-falling models were the temperature threshold model, photoperiod threshold model, cold-degree-day photoperiod-dependent model, and a new scheme called summer-influenced autumn (SummerIA) model proposed in this study. The scientific questions addressed in this study included: (a) Which kind of model has the best performance in simulating the leaf unfolding dates and leaf falling dates for deciduous forests? (b) Whether the modification of phenology models will improve the simulation of carbon uptake duration, amplitude, and gross primary productivity (GPP)? (c) How does the modified phenology model predict the changes of phenological dates of deciduous forests and its regional variations in response to climate warming in China during 2016–2100?

We first evaluated and modified the performance of four leaf-unfolding models and four leaf-falling models using observed phenology data during 2003–2015 at the five sites of CERN. The five forest sites included the Changbaishan temperate broad-leaved Korean pine mixed forest (CBF), Beijing warm temperate secondary deciduous broad-leaved forest (BJF), Maoxian subalpine coniferous forest (MXF), Shennongjia subtropical evergreen deciduous broad-leaved mixed forest (SNF), and Gonggashan coniferous broad-leaved mixed forest (GGF). Second, the best leaf-unfolding and leaf-falling models were also validated by observed phenology data at eight sites of Chinese Phenological Observation Network (CPON) (Ge et al., 2014, 2015; H. Wang et al., 2014, 2015), and GIMMS-derived phenology data in 1982–2014. Third, we examined the ability of CLM4.5 with modified deciduous phenology submodels in simulating GPP, carbon uptake duration, and carbon uptake amplitude at CBF and five forest sites from FLUXNET due to the limitation of flux observation for deciduous forests in CERN. Finally, we predicted phenology changes in China's deciduous forests during 2016–2100 using the modified phenology models.

2. Materials and Methods

2.1. Study Region

The study region covers all deciduous forests in China, including deciduous broad-leaved forests, deciduous needle-leaved forests, and mixed forests, which account for 14.72%, 2.90%, and 2.33% of China's forests, respectively (Figure 1). The deciduous forest map was extracted from the China land cover data set (Wu et al., 2014), which was produced using Landsat TM/ETM and HJ-1 satellite data of 30 m resolution in 2010, combined with a large amount of data of field investigation. The deciduous forests are mainly located in the temperate climate zone with the percentage of 67%, followed by the subtropical climate zone (18%), and the cold temperate climate zone (15%), according to the China's climate zone data downloaded from the Resource and Environmental Science Data Center of the Chinese Academy of Sciences (<http://www.resdc.cn/>).

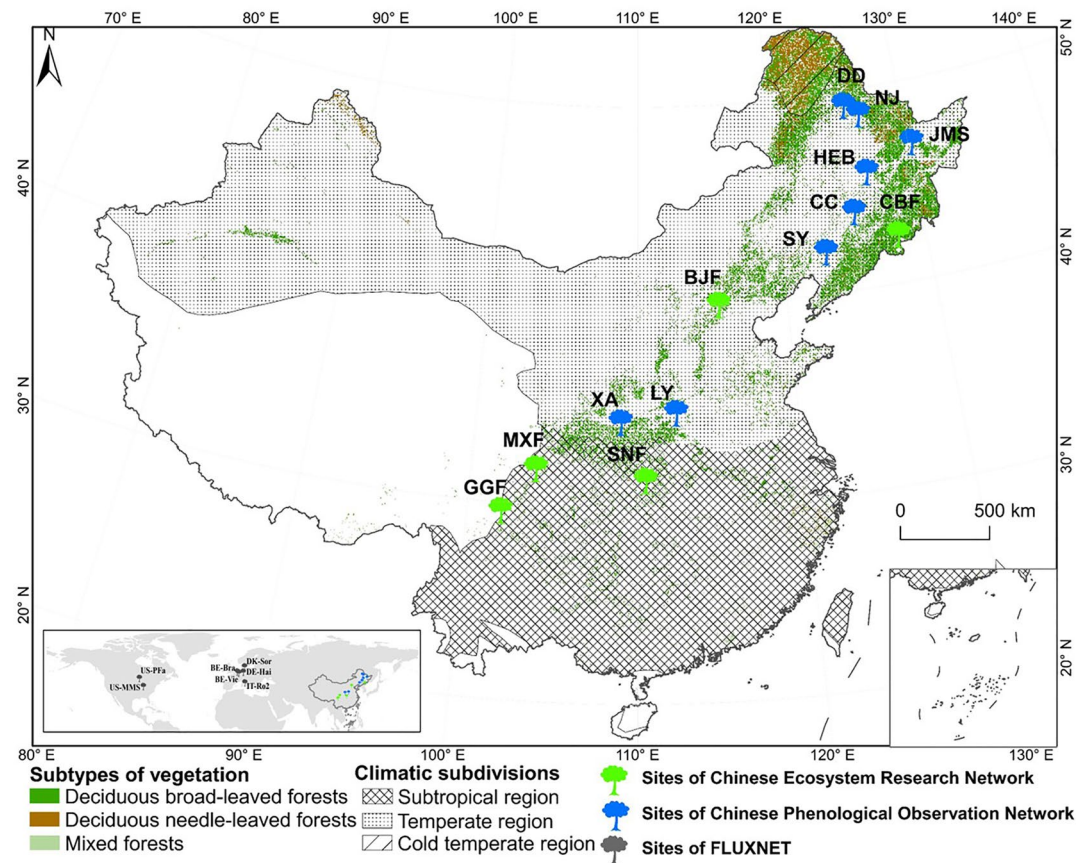


Figure 1. Description of observation sites. Green: five forest sites of the Chinese Ecosystem Research Network (CERN), Blue: eight forest sites of the Chinese Phenological Observation Network (CPON), and Black: five forest sites of FLUXNET. Transverse stripe: the subtropical region, scatter: the temperate region, and diagonal stripe: the cold temperate region. Dark green: the deciduous broad-leaved forests, Brown: the deciduous needle-leaved forests, and Light green: the mixed forests.

2.2. Data

2.2.1. Climate Data

To compare the performance of four leaf-unfolding models and four leaf-falling models at the five sites of CERN, we collected observed hourly air temperature data during 2003–2015 (<http://www.cern.org.cn/>) to drive the phenological models. Hourly meteorological data at each site were gap-filled using observations made from the CERN data set (<http://www.cern.org.cn/>).

For the model evaluation at the eight CPON sites (i.e., Nenjiang, Dedu, Jiamusi, Haerbin, Changchun, Shenyang, Luoyang and Xian), daily air temperature data were collected from the neighboring meteorological stations of China Meteorological Administration (<http://data.cma.cn>) to drive the phenological models.

Hourly meteorological data were collected at CBF and five FLUXNET sites (i.e., BE-Bra, BE-Vie, US-PFa, IT-Ro2, and US-MMS) to drive CLM4.5 for investigating the improvement of phenology simulation on GPP modeling. Hourly meteorological data included the downwelling long-wave radiation (W/m^2), downwelling short-wave radiation (W/m^2), air temperature (K), precipitation (mm/s), relative humidity (%), surface pressure (Pa), and wind speed (m/s). The hourly meteorological data at CBF during 2003–2008 were obtained from CERN data set (<http://www.cern.org.cn/>). We also collected the hourly meteorological data at five forest sites from FLUXNET due to the limited number of available sites in China's deciduous forests. The selection of the forest site from FLUXNET followed three criteria. The deciduous broadleaf forests have similar environmental conditions to China's deciduous forests. The proportion of missing data of observed GPP is less than 20%. And these sites have 10 or more years of data. The brief descriptions of site characteristic are shown in Table 1.

Table 1
Site Characteristics of Five Forest Sites of Chinese Ecosystem Research Network (CERN), Eight Forest Sites of Chinese Phenological Observation Network (CPON), and Five Forest Sites of FLUXNET

Network	Site	Dominant deciduous tree	Latitude/N	Longitude/E	Elevation/m	Annual mean temperature/°C	Annual total precipitation/mm	Period
CERN	Changbaishan (CBF)	<i>Acer mono</i>	42.40	128.09	784	3.62 ± 0.65	712.30 ± 22.37	2003–2015, 2003–2008 ^a
	Beijing (BJF)	<i>Quercus wutaishanica</i>	39.96	115.43	1,263	5.20 ± 0.49	427.88 ± 70.66	2003–2015
	Maoxian (MXF)	<i>Quercus aliena</i> var. <i>Acuteserrata</i>	31.78	103.88	1,816	9.47 ± 0.41	716.86 ± 105.34	2005–2015
	Shennongjia (SNF)	<i>Quercus serrata</i> var. <i>brevipetiolata</i>	31.32	110.5	1,750	10.32 ± 0.47	1,150.67 ± 98.59	2009–2015
	Gonggashan (GGF)	<i>Betula utilis</i>	29.57	101.99	3,160	5.22 ± 0.44	1,653.00 ± 164.36	2005–2015
CPON	Nenjiang (NJ)	<i>Larix gmelinii</i> , <i>Acer mono</i>	49.25	125.75	281	0.40 ± 0.70	550.30 ± 91.89	1986–1991, 1993–1996
	Dedu (DD)	<i>Larix gmelinii</i> , <i>Acer negundo</i>	48.7	126.75	324	0.50 ± 0.62	562.08 ± 97.26	1986–1991, 1993–1996
	Jiamusi (JMS)	<i>Acer negundo</i>	46.82	130.28	80	3.10 ± 0.61	602.14 ± 107.44	1986, 1988–1996
	Haerbin (HEB)	<i>Betula platyphylla</i> , <i>Acer ginnala</i> , <i>Larix gmelinii</i> , <i>Quercus acutissima</i>	45.75	126.67	146	4.00 ± 0.62	547.99 ± 101.91	1986–1991, 2003–2008
	Changchun (CC)	<i>Betula platyphylla</i> , <i>Acer ginnala</i> , <i>Larix gmelinii</i> , <i>Quercus mongolica</i> , <i>Acer truncatum</i>	43.87	125.33	215	5.90 ± 0.63	602.49 ± 116.10	1986–1991, 1993–1994, 2003–2008
	Shenyang (SY)	<i>Betula platyphylla</i> , <i>Acer ginnala</i> , <i>Larix gmelinii</i> , <i>Acer truncatum</i>	42.08	123.00	53	8.20 ± 1.58	602.51 ± 132.59	2003–2008, 2013–2014
	Luoyang (LY)	<i>Populus tomentosa</i>	34.67	112.42	138	15.40 ± 0.55	603.64 ± 121.31	1986, 1988–1996
	Xian (XA)	<i>Betula platyphylla</i> , <i>Quercus variabilis</i> , <i>Acer mono</i>	34.22	108.97	436	13.40 ± 0.62	642.53 ± 112.88	1986, 1988, 1990, 1993–1994, 1996, 2003–2008
FLUXNET	BE-Bra	<i>Larix gmelinii</i> (Rupr.) Kuzen	51.30	4.52	16	9.80 ± 0.74	750.00 ± 141.08	1996–2014
	BE-Vie	Douglas fir, <i>Pseudotsuga sinensis</i>	50.31	6.00	493	7.80 ± 0.67	1,062.00 ± 195.62	1996–2014
	US-PFa	<i>Pinus koraiensis</i> , <i>Pinus banksiana</i>	45.95	-90.27	470	4.33 ± 1.32	823.00 ± 132.29	1995–2014
	IT-Ro2	<i>Quercus cerris</i> L.	42.39	11.92	160	15.15 ± 0.68	876.00 ± 253.27	2002–2012
	US-MMS	<i>Acer tonkinense</i> subsp. <i>Fagales</i>	39.32	-86.41	275	10.85 ± 0.81	1,032.00 ± 188.16	1999–2014

^aRepresents the period of GPP data at CBF.

Table 2
Descriptions of the Four Leaf Unfolding Models With Three Expressions of Chill Accumulation

Models	CU	Tcbase (°C)	Tfbase (°C)	The start day of CU	The end day of CU	The start day of FU
Spring warming model	No	—	$T > 0$	—	—	The winter solstice of the previous year
Sequential CU1 model	Yes	$T \leq 5$	$T > 0$	1 November of the previous year	1 February	1 February
Sequential CU2 model		$0 \leq T \leq 5$				
Sequential CU3 model		$-3.4 < T < 10.4$				
Parallel CU1 model	Yes	$T \leq 5$	$T > 0$	1 November of the previous year	Leaf unfolding date	1 November of the previous year
Parallel CU2 model		$0 \leq T \leq 5$				
Parallel CU3 model		$-3.4 < T < 10.4$				
Alternating CU1 model	Yes	$T \leq 5$	$T > 5$	1 November of the previous year	Leaf unfolding date	1 November of the previous year
Alternating CU2 model	Yes	$0 \leq T \leq 5$	$T > 5$			
Alternating CU3 model	Yes	$-3.4 < T < 10.4$	$T \geq 10.4$			

Note. CU is the chill accumulation. FU is the heat requirement. T is the mean temperature (°C) in each time step. Tcbase is the base temperature for chill accumulation (°C). Tfbase is the base temperature for heat requirement (°C). Tcbase is equal to Tfbase in alternating model, while Tcbase is different to Tfbase in the other models.

We also collected regional air temperature data to drive the phenological models for evaluating the modified phenology models at the regional scale in 1981–2015 and investigating the phenological changes in China's deciduous forest in the period of 2016–2100. The temperature data from 1981 to 2015 were collected from the China Meteorological Forcing Data set with a time resolution of 3 hr and a spatial resolution of 0.1° (He et al., 2020) and then were averaged to the daily scale. For the prediction in 2016–2100, we used daily temperature data in the RCP4.5 scenario, because the trend of emission, concentration, and radiation forcing time of the three major greenhouse gases in the RCP4.5 scenario are relatively consistent with China's future economic development and suitable for China's national conditions (Gao et al., 2014). The daily temperature data in the RCP4.5 scenario were obtained from the Global Daily Downscaled Projections (NEX-GDDP-CMIP6), which was the ensemble mean value of 30 models (Table S4 in Supporting Information S1), with a time resolution of 1 day and a spatial resolution of 0.25° (Thrasher et al., 2022).

2.2.2. Phenology Data

Observed phenological data of the dominant deciduous trees at five sites in CERN (i.e., CBF, BJF, MXF, SNF, and GGF) during 2003–2015 (Song et al., 2017) were used to modify and validate the deciduous phenology models.

We also collected the phenological observations at the eight CPON forest sites (i.e., Nenjiang, Dedu, Jiamusi, Haerbin, Changchun, Shenyang, Luoyang and Xian) of CPON (Ge et al., 2014, 2015; H. Wang et al., 2014, 2015) to evaluate the deciduous phenology models with best performance. Observed phenological dates at eight typical deciduous forest sites of CPON were downloaded from the National Earth System Science Data Sharing Platform (<http://www.geodata.cn>). We averaged leaf unfolding and leaf falling dates for dominant species at each deciduous forest site in CPON.

At the regional scale, we used a GIMMS (global inventory modeling and mapping studies) Phenology data set in 1982–2014 produced by X. Wang et al. (2019) to evaluate phenology predictions in China's deciduous forests estimated by modified phenology models. The start and end of growing season dates were estimated from the time series of GIMMS NDVI (Normalized Difference Vegetation Index) using the inflection point detection method (X. Wang et al., 2017). Specially, the start and end of growing season were determined as the date corresponding to the maxima (or minima) value in first-order derivative of the fitted double logistic curve of NDVI time series. We resampled the GIMMS Phenology data set to 0.1°.

2.2.3. GPP Data Estimated by Eddy Covariance Measurements

Eddy-covariance fluxes were used to investigate the influence of phenology changes on carbon flux simulated with the CLM4.5 model. Among the five forest sites of CERN, eddy-covariance fluxes were simultaneously measured at the CBF site. The observed GPP at CBF during 2003–2008 were obtained from the ChinaFLUX data set (<http://www.chinaflux.org/>). We also collected eddy-covariance data from the five sites in FLUXNET (i.e., BE-Bra, BE-Vie, US-PFa, IT-Ro2, and US-MMS), which were obtained from the FLUXNET database released in 2015 (Pastorello et al., 2020).

2.3. Models

2.3.1. Leaf Unfolding Models

We compared four leaf unfolding models (i.e., the spring warming model, sequential model, parallel model, and alternating model) to examine to what extent the involvement of cold temperature can improve the performance of leaf unfolding dates modeling and what kind of assumption on dormancy (i.e., the rest and quiescence exist sequential, parallel, or alternative) has the best performance (Table 2). Leaf unfolding is assumed to occur when heat requirement exceeds the threshold that is expressed by the function of

chill accumulation in the sequential model, parallel model, alternating model, and by that of mean air temperature in the spring warming model.

In the spring warming model, the rate of heat requirement follows a logistic function of temperature (Chuine et al., 1998; Hänninen, 1990). Leaf appears after a certain amount of accumulated heat requirement. This model is the simplest model of leaf unfolding prediction, which has been used in CLM4.5.

$$FU_1 = \sum_{t_0}^{t_{\text{pheno}}} \begin{cases} \frac{28.4}{1+e^{(3.4-0.185 \cdot T)}} & T > 0 \\ 0 & T \leq 0 \end{cases} \quad (1)$$

where FU_1 is the rate of heat requirement, and T is mean temperature ($^{\circ}\text{C}$) in each time step. The dates of t_0 and t_{pheno} are winter solstice of the previous year and leaf unfolding date, respectively. The critical threshold (FU_{cirt}) of forcing accumulation required for leaf unfolding is as follows.

$$FU_{\text{cirt}} \geq e^{a+b \cdot T_{\text{ann}}} \quad (2)$$

where T_{ann} is the annual average temperature in the previous year. Estimated coefficients a and b are 4.8 and 0.13, respectively, in original deciduous phenological submodel in CLM4.5 (Oleson et al., 2013).

The sequential model assumes that rest and quiescence are two strictly separate periods, with no response to warm temperatures before rest release (Sarvas, 1972, 1974). Heat requirement is not active as long as chill accumulation is not reached. The most commonly used temperature threshold of 5°C (Cannell & Smith, 1983; Y. H. Fu et al., 2015) is applied in CU_1 .

$$CU_1 = \sum_{t_0}^{t_1} \begin{cases} 1 & T \leq 5 \\ 0 & T > 5 \end{cases} \quad (3)$$

$$FU_1 = \sum_{t_1}^{t_{\text{pheno}}} \begin{cases} \frac{28.4}{1+e^{(3.4-0.185 \cdot T)}} & T > 0 \\ 0 & T \leq 0 \end{cases} \quad (4)$$

where CU_1 is the rate of chill accumulation, FU_1 is the rate of heat requirement, and T is mean temperature ($^{\circ}\text{C}$) in each time step. The dates of t_0 , t_1 , and t_{pheno} are 1 November of the previous year, 1 February, and leaf unfolding date, respectively.

In the parallel model, rest and quiescence occur simultaneously; even when the rest has not yet been attained, a response to warm temperatures must be possible (Landsberg, 1974). Heat requirement can be active concomitant with the time spent for chill accumulation.

$$CU_1 = \sum_{t_0}^{t_{\text{pheno}}} \begin{cases} 1 & T \leq 5 \\ 0 & T > 5 \end{cases} \quad (5)$$

$$FU_1 = \sum_{t_0}^{t_{\text{pheno}}} \begin{cases} \frac{28.4}{1+e^{(3.4-0.185 \cdot T)}} & T > 0 \\ 0 & T \leq 0 \end{cases} \quad (6)$$

where CU_1 is the rate of chill accumulation, FU_1 is the rate of heat requirement, and T is mean temperature ($^{\circ}\text{C}$) in each time step. The dates of t_0 and t_{pheno} are 1 November of the previous year and leaf unfolding date, respectively.

In the alternating model, the rest and quiescence exist alternately, and chill accumulation and heat requirement take turns from a start date relative to a base temperature (Cannell & Smith, 1983). There is only one temperature threshold of heat requirement and chill accumulation in the alternating model. When the temperature is

lower than the temperature threshold, chill accumulation occurs as Equation 5. Otherwise, heat requirement starts to accumulate as Equation 7.

$$FU_1 = \sum_{t_0}^{t_{\text{pheno}}} \begin{cases} \frac{28.4}{1+e^{(3.4-0.185 \cdot T)}} & T > 5 \\ 0 & T \leq 5 \end{cases} \quad (7)$$

where FU_1 is the rate of heat requirement, and T is mean temperature ($^{\circ}\text{C}$) in each time step. The dates of t_0 and t_{pheno} are 1 November of the previous year and leaf unfolding date, respectively.

The other two expressions of chill accumulation (i.e., CU_2 and CU_3) and another expression of heat requirement (FU_2) were also compared in different leaf unfolding dates models to estimate the effects of different expression of chill accumulation and heat requirement on model performance. The calculation of chilling accumulation in CU_2 was the same as that in CU_1 but with different specific temperature thresholds. In CU_2 , it is assumed that freezing temperatures do not contribute to winter chill accumulation (Y. H. Fu et al., 2015; Peaucelle et al., 2019), and $0\text{--}5^{\circ}\text{C}$ is regarded as the effective temperature range for chill accumulation.

$$CU_2 = \sum \begin{cases} 1 & 0 \leq T \leq 5 \\ 0 & T < 0, \text{ or } T > 5 \end{cases} \quad (8)$$

In model CU_3 , the chill accumulation is expressed by a triangular form, which is fitted by Hänninen (1990) using previous experimental results for Finnish birch seedlings. The effective temperature range for chill accumulation in CU_3 is -3.4 to 10.4°C .

$$CU_3 = \sum \begin{cases} 0 & T \geq 10.4 \text{ or } T \leq -3.4 \\ \frac{T+3.4}{6.9} & -3.4 < T < 3.5 \\ \frac{T-10.4}{(-6.9)} & 3.5 < T < 10.4 \end{cases} \quad (9)$$

In the other forcing model FU_2 , the heat requirement is accumulated when it is above a particular threshold (i.e., 0°C) as in previous studies (Basler & Koerner, 2012; Heide, 1993; Piao et al., 2015).

$$FU_2 = \sum \begin{cases} T & T > 0 \\ 0 & T \leq 0 \end{cases} \quad (10)$$

where FU_2 is the rate of forcing, and T is the mean temperature ($^{\circ}\text{C}$) in each time step.

Leaf unfolding dates occur when heat requirement exceeds the threshold that is expressed by the function of chill accumulation in the sequential model, parallel model, and alternating model.

$$FU_{\text{crit}} \geq \begin{cases} a + b \cdot e^{-c \cdot CU_1} & CU_1 \\ e^{(a+b \cdot CU)} & CU_{2,3} \end{cases} \quad (11)$$

Constant coefficients (i.e., a , b , and c) for calculating the threshold of leaf unfolding dates in Equation 11 were estimated by the least square method using the observed phenological data across the five CERN sites in 2005–2012 (30 site years) (Figure 2).

2.3.2. Leaf Falling Models

Four leaf falling models were compared in this study, including the temperature threshold model, photoperiod threshold model, cold-degree-day photoperiod-dependent model (CDD/P) and SummerIA model hereinafter referred to as T , PT , CDD/P , and $SummerIA$, respectively (Table 3).

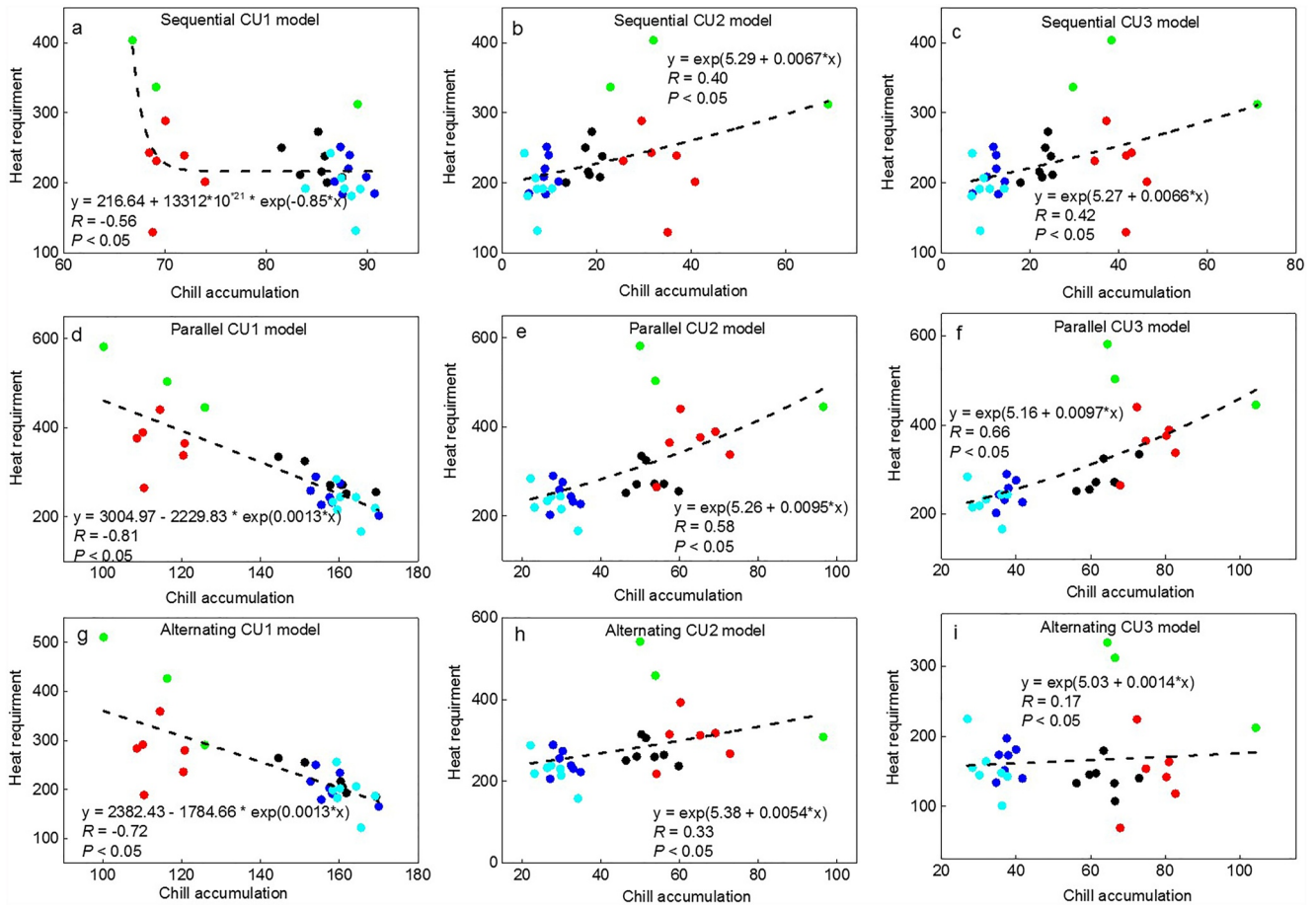


Figure 2. Relationship between chill accumulation and heat requirement for leaf unfolding dates across five Chinese Ecosystem Research Network (CERN) forest sites. Green: Shennongjia subtropical evergreen deciduous broad-leaved mixed forest (SNF), Red: Maoxian subalpine coniferous forest (MXF), Black: Gonggashan coniferous broad-leaved mixed forest (GGF), Dark blue: Beijing warm temperate secondary deciduous broad-leaved forest (BJF), and Light blue: Changbaishan temperate broad-leaved Korean pine mixed forest (CBF).

In the T model, the leaves fall when the temperature is less than 5°C after the summer solstice (Chuine et al., 2013). In the PT model, the leaves fall when the photoperiod is less than 39,300 s (10.91 hr) after the summer solstice as in CLM4.5 (White et al., 1997).

The CDD/P model was originally used to simulate the discoloration of the blade and was further applied to the simulation of blade senescence. Leaves fall is postulated to be the result of continuous senescence processes after the summer solstice (Archetti et al., 2013; Delpierre et al., 2009; Vitasse et al., 2011). We defined aging state (S_{sen}) of each day less than the photoperiod threshold P_{start} (Equation 12), represented by the daylength-sensitive cold-degree day summation (Equations 13 and 14). The accumulation of aging state varies with latitude according to the photoperiod parameter P_{start} . When S_{sen} reached the threshold (Y_{crit}) the leaves began to fall.

Table 3
Descriptions of the Four Leaf Falling Models

Models	Tbase ($^{\circ}\text{C}$)	Pbase (hr)	Aging state threshold	The start day of aging state	The end day of aging state
T model	$T < 5$	–	–	–	–
PT model	–	$P < 10.91$	–	–	–
CDD/P model	$T < 14.5$	$P < 14.5$	414.84	The summer solstice	Leaf falling date
SummerIA model	$T < 14.5$	$P < 14.5$	The function of summer temperature	–	–

Note. T is the mean temperature ($^{\circ}\text{C}$) in each time step. Tbase is the base temperature ($^{\circ}\text{C}$). Pbase is the base photoperiod (hr).

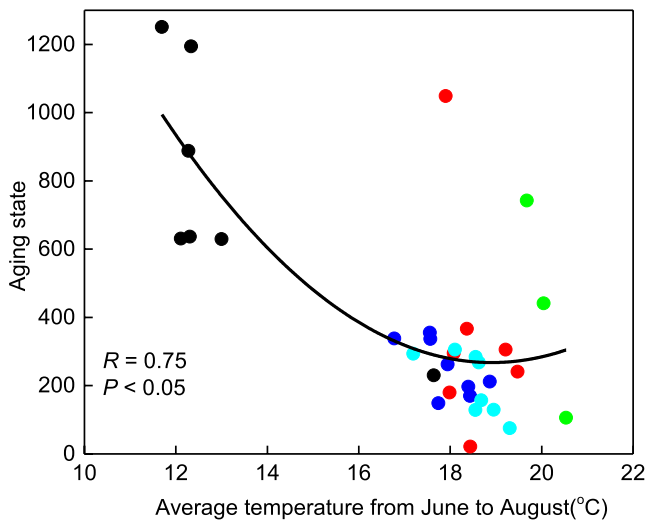


Figure 3. Relationship between observed aging state and mean temperature from June to August across five Chinese Ecosystem Research Network (CERN) forest sites. Green: Shennongjia subtropical evergreen deciduous broad-leaved mixed forest (SNF), Red: Maoxian subalpine coniferous forest (MXF), Black: Gonggashan coniferous broad-leaved mixed forest (GGF), Dark blue: Beijing warm temperate secondary deciduous broad-leaved forest (BJF), Light blue: Changbaishan temperate broad-leaved Korean pine mixed forest (CBF).

temperature, photoperiod, and leaf falling dates in the five CERN forest sites to calculate the observed aging state. Our results show that the observed aging state significantly decreased with the average temperature from June to August (Figure 3). Thus, we developed a SummerIA model in this study based on the CDD/P model using a nonlinear function of threshold instead of a constant value.

$$S_{\text{sen}}(d) \geq Y_{\text{crit}} = a \cdot T_{\text{summer}} \cdot T_{\text{summer}} + b \cdot T_{\text{summer}} + c \quad (16)$$

where T_{summer} is the average temperature from June to August. a , b , and c are 13.98, -528.62 , and $5,264.90$, respectively. Constant coefficients for calculating the threshold of leaf falling dates in Equation 14 were estimated by the least square method using the observed phenological data across five CERN sites in 2005–2012 (30 site years).

2.3.3. CLM4.5

The CLM4.5 model simulates biogeophysical and bio-geochemical processes in the atmosphere—vegetation—soil continuum (Oleson et al., 2013). In the past few years, the CLM4.5 model has been evaluated and well applied in China (Jia et al., 2018; P. Li et al., 2018; Lv et al., 2023; Xue et al., 2021; Zhang et al., 2016). Based on the evaluation of different deciduous phenological models, the deciduous submodel in CLM4.5 were modified using the alternating CUI model and SummerIA model to simulate the spring leaf-out and autumn leaf fall, respectively. We then simulated the phenological dates and carbon fluxes using CLM4.5 with original phenological models and modified phenological models in our study at CBF from 2003 to 2008, at BE-Bra in 1996–2014, at BE-Vie in 1996–2014, at US-PFa in 1995–2014, at IT-Ro2 in 2002–2012, and at US-MMS in 1999–2014. We ran CLM4.5 at hourly time steps.

2.4. Statistic Analysis

2.4.1. Model Assessment

The observed phenological data during 2013–2015 across the five CERN sites (15 site years) were used to evaluate phenological models. The observed phenological data across the eight typical deciduous forest sites of CPON during 1981–2008 (78 site years) were also used to evaluate phenological models. Here, we used the correlation

$$S_{\text{sen}}(d) = \begin{cases} 0, & P(d) \geq P_{\text{start}} \\ S_{\text{sen}}(d-1) + R_{\text{sen}}(d), & P(d) < P_{\text{start}} \end{cases} \quad (12)$$

$$R_{\text{sen}}(d) = \begin{cases} [T_b - T(d)]^x \cdot f[P(d)]^y, & T(d) < T_b \\ 0, & T(d) \geq T_b \end{cases} \quad (13)$$

The calculation function of the effect of photoperiod on leaf falling dates is:

$$f[P(d)] = \frac{P(d)}{P_{\text{start}}} \quad (14)$$

The threshold is calculated as:

$$S_{\text{sen}}(d) \geq Y_{\text{crit}} \quad (15)$$

where $P(d)$ is the photoperiod, P_{start} is the photoperiod when the blade begins to age (14.5 hr), T_b is the temperature at which the blade begins to age (14.5°C), and $f[P(d)]$ is the photoperiod function. The parameters x and y are 2, and the threshold Y_{crit} is 414.84.

Since leaf falling dates were found to be affected by the temperature over a few months prior to the leaf falling dates ago (Estrella and Menzel, 2006), we analyzed the relationship between observed aging state and average temperature in summer across the five CERN forest sites. We used the observed

Table 4

Comparison of Simulation Results Among Different Combinations of Three Chilling Models and the FU1 Model and Spring Warming Model Across the Five Chinese Ecosystem Research Network (CERN) Forest Sites

	<i>R</i>	RMSE (day)	MBE (day)	MRE (%)	AICc
Spring warming model	0.62	8	9	4.51	6.07
Sequential CU1 model	0.65	8	6	5.14	5.86
Sequential CU2 model	0.58	11	9	1.76	6.21
Sequential CU3 model	0.58	11	9	2.21	6.16
Parallel CU1 model	0.80	6	6	2.79	5.40
Parallel CU2 model	0.80	13	10	-3.39	6.55
Parallel CU3 model	0.82	12	10	-2.27	6.29
Alternating CU1 model	0.81	7	6	-1.10	5.23
Alternating CU2 model	0.77	13	10	-2.93	6.51
Alternating CU3 model	0.72	12	8	-2.43	6.03

coefficient (*R*), root Mean Squared Error (RMSE), mean bias error (MBE), relative error (MRE), and Akaike information criterion (corrected for small samples, AICc) to evaluate the model's behaviors. AICc was used to evaluate the trade-offs between different methods in model simplicity and goodness of fit (Burnham & Anderson, 2002). The formula for AICc is as follows:

$$AIC_c = \ln\left(\frac{sse}{n}\right) + \frac{(n+k)}{(n-k-2)} \quad (17)$$

where *k* is the number of parameters, *n* is the sample size, and sse is the sum of squared residuals. The smaller the AICc value is, the better the interpretation of the data is.

2.4.2. Calculation of Carbon Uptake Duration and Carbon Uptake Amplitude

Based on the daily GPP data in eight forest sites (e.g., CBF, DK-Sor, BE-Bra, DE-Hai, BE-Vie, US-PFa, IT-Ro2, and US-MMS), we used the method put forward by L. Gu et al. (2009) to determinate the carbon uptake duration. The starting date and ending date of carbon uptake can be located by calculating the radius of curvature of daily photosynthetic rates. For a given point on a curve, the radius of curvature is the radius of the circle that fits the curve at

that point. The starting date of carbon uptake was the date when canopy photosynthesis development starts to accelerate in response to the rapid improvement in meteorological conditions for plant growth, while the ending date of carbon uptake was the date when canopy photosynthesis enters into a period of quick decline in response to the deterioration in meteorological conditions for plant growth. The carbon uptake duration was the number of days between the starting date and ending date of carbon uptake. The carbon uptake amplitude is the maximum value of the monthly land carbon sink (Xia et al., 2015).

2.4.3. Temperature Sensitivity of Leaf Unfolding and Leaf Falling Dates

The detrended anomaly has been widely used to analyze the variation and to calculate the sensitivity of a variable to temperature, precipitation, and other environmental factors (Piao et al., 2013; H. Wang et al., 2015; Zhang et al., 2019), because detrending can remove the trend of data. Here we conducted a linear regression analysis between detrended anomaly of leaf unfolding or leaf falling dates and detrended anomaly of mean air temperature. The regression coefficient was defined as the temperature sensitivity of leaf unfolding or leaf falling dates. The detrended anomaly was the difference between the values of a variable and the predicted values from the regression model between the variable and time (i.e., year) in this study (Equations S1 and S2 in Supporting Information S1).

3. Results

3.1. Evaluation of Deciduous Phenological Models Against Observations at CERN Sites

Compared with observations, the parallel model and alternating model had better performance in simulating leaf unfolding dates than the spring warming model and the sequential model. Pearson's correlation coefficients between modeled and observed values of leaf unfolding dates across the five CERN forest sites in the parallel model and alternating model ranged from 0.72 to 0.82, larger than that in the spring warming model (0.62) and sequential model (0.58–0.65). MRE values of the parallel model and alternating model (-3.39% to -1.10%) were less than those of the sequential model (1.76%–5.14%) and spring warming model (4.51%) (Table 4). Table 4 provides a summary of the best-fit leaf unfolding dates models and their relative performance given the forcing model FU1. When using the forcing model FU2, modeled leaf unfolding dates based on FU2 were highly correlated with those based on FU1 (Table S2 in Supporting Information S1), and the results on performance of these above leaf unfolding date models were consistent with those with FU1 (Table S3 in Supporting Information S1).

Among the three chilling models, CU1 performed the best with the lowest values of RMSE, MBE, and AICc in the sequential model, parallel model, and alternating model (Table 4). The parallel CU1 model and alternating CU1 model showed comparatively good performance across the five CERN forest sites. Further evaluation on

Table 5

Assessment of Two CU1 Models (i.e., the Parallel CU1 Model and Alternating CU1 Model) at the Five Forest Sites of the Chinese Ecosystem Research Network (CERN)

	Parallel CU1 model			Alternating CU1 model		
	RMSE (day)	MBE (day)	MRE (%)	RMSE (day)	MBE (day)	MRE (%)
CBF	5	5	2.59	4	4	-2.32
BJF	4	10	8.83	4	5	4.60
GGF	2	2	-1.12	1	3	-2.48
MXF	2	8	7.37	1	6	3.29
SNF	1	4	-3.73	2	10	-8.59

modeled leaf unfolding dates between these two CU1 models at each forest site was shown in Table 5. The alternating CU1 model had higher consistency with the observed leaf unfolding dates with lower RMSE (1–4 days), MBE (3–6 days), and MRE (-2.48% to 4.60%) than the parallel CU1 model at CBF, BJF, GGF, and MXF. But the alternating CU1 model showed poor behavior in simulating leaf unfolding dates at SNF.

Among the four leaf falling models, the SummerIA model showed the best performance in simulating leaf falling date at the five CERN forest sites. The PT model had a relatively low Pearson's correlation coefficient of 0.57 and the largest MBE of 28 days. The commonly used *T* model had a high Pearson's correlation coefficient of 0.93 but a relatively large MBE of 18 days. Although the CDD/P model considers the effects of both photoperiod and temperature, it still had a large MBE of 19 days (Table 6). The SummerIA model showed the lowest AICc value of 6.98 across the five CERN forest sites. Compared with the other three models, the SummerIA model also had the lowest RMSE, MBE, and MRE at three of the five forest sites (i.e., CBF, BJF, and GGF; Table 7).

3.2. Evaluation of Modified Phenological Model Against Observations From CPON and GIMMS Data

Compared with original CLM4.5 (referred as to CLM4.5_old), modified CLM4.5 (referred as to CLM4.5_new) had a better performance in simulating the leaf unfolding dates and leaf falling dates. Specifically, the MBE values of modeled leaf unfolding dates were reduced by 5 days in CLM4.5_new except for the LY site, when compared with CLM4.5_old (Figure 4a). For the leaf falling dates, CLM4.5_new had lower MRE values (-2.46% to 7.26%) than CLM4.5_old (-2.72% to 10.66%) except for the XA site (Figure 4b).

Based on the GIMMS-derived leaf unfolding and leaf falling dates, CLM4.5_new showed a better ability to simulate the spatial pattern and temporal variation in leaf unfolding and leaf falling dates than CLM4.5_old (Figure 5). Both CLM4.5_old and CLM4.5_new could reproduce the regional variation in leaf unfolding dates, leaf falling dates, and growing season length compared to GIMMS-derived phenology (Figure 5). However, CLM4.5_new showed better consistency in phenology with GIMMS-NDVI3g than CLM4.5_old (Figure 6a). The bias of mean leaf unfolding dates and leaf falling dates were reduced from -14 and 21 days in CLM4.5_old to -3 and 9 days in CLM4.5_new, respectively.

Moreover, the trend of leaf unfolding predictions from CLM4.5_new (-0.20 days/year) was more consistent with GIMMS-derived trend (-0.17 days/year) than that from CLM4.5_old (-0.12 days/year; Figure 6b). In contrast to CLM4.5_old with constant leaf falling dates or no trend, CLM4.5_new agreed with GIMMS-NDVI3g in the delayed trend of leaf falling date during 1982–2014 (Figure 6b). Consequently, CLM4.5_new well presents the temporal changes of growing season length in China's deciduous forests (Figure 6b). The trend difference in growing season length between GIMMS-NDVI 3g and model decreased from 0.24 days/year in CLM4.5_old to 0.08 days/year in CLM4.5_new.

Across all China's deciduous forests, CLM4.5_new also well simulated the coefficient of variation (CV) of leaf falling and growing season length (Figure 6c). The CV of leaf falling dates (0.91%) for CLM4.5_new was close to that (1.23%) for GIMMS-NDVI3g. The differences between predicted and GIMMS-derived growing season length CV for CLM4.5_new (1.41%) was lower than that for CLM4.5_old (2.36%).

Table 6

Comparison of Simulation Results Among Different Leaf Falling Dates Models Across the Five Chinese Ecosystem Research Network (CERN) Forest Sites

	<i>R</i>	RMSE (day)	MBE (day)	MRE (%)	AICc
<i>T</i> model	0.93	6	18	5.51	7.43
PT model	0.57	5	28	6.72	8.14
CDD/P model	0.53	20	19	0.37	7.67
SummerIA model	0.92	6	14	-1.75	6.98

3.3. Effects of Phenology Improvement on GPP Simulation

The results showed that the modification of phenology models increased the prediction accuracy of annual GPP and its interannual variation (IAV). Compared with CLM4.5_old, MRE values of annual GPP simulated by

Table 7
Assessment of Modeled Leaf Falling Dates at the Five Forest Sites Within Chinese Ecosystem Research Network (CERN)

	T model			PT model			CDD/P model			SummerIA model		
	RMSE (day)	MBE (day)	MRE (%)	RMSE (day)	MBE (day)	MRE (%)	RMSE (day)	MBE (day)	MRE (%)	RMSE (day)	MBE (day)	MRE (%)
CBF	1	22	8.30	–	31	11.82	2	9	3.49	1	3	1.12
BJF	2	31	12.19	–	36	13.98	3	38	14.74	9	14	–4.61
GGF	7	21	7.80	–	40	14.91	–	19	–10.48	2	8	–0.75
MXF	7	8	–2.33	–	18	–5.39	–	17	–5.23	4	24	–7.51
SNF	7	5	1.61	–	5	–1.69	5	13	–4.26	3	20	–6.27

CLM4.5_new were reduced from –25% to 26% to –14% to 11% across the six sites (Figure 7a). Meanwhile, the CV of annual GPP reproduced by CLM4.5_new was well consistent with observed values at BE-Bra, BE-Vie, IT-Ro2, and CBF (Figure 7b).

The improvement of modeled annual GPP due to the modification of phenology was mainly caused by better prediction on the carbon uptake duration and carbon uptake amplitude (Figures 7c and 7d). The reduction of annual GPP bias modeled by CLM4.5_new at BE-Bra and CBF was mainly associated with the diminished over-estimation of carbon uptake duration by 6–19 days. Consequently, modeled GPP from the date of carbon uptake amplitude to the end of carbon uptake duration at CBF decreased by 13.31%, when compared with CLM4.5_old. Modeled GPP from the start of carbon uptake amplitude to the date of carbon uptake duration at BE-Bra decreased by 15.16% comparing to CLM4.5_old. CLM4.5_new reduced the bias of leaf falling dates by 11 days at US-PFa. For the BE-Vie and US-MMS sites, CLM4.5_new reduced the bias of leaf unfolding dates by 7 and 22 days, respectively. Simultaneously, the bias of modeled carbon uptake amplitude was reduced from –3.92 and –6.33 gC/m²/day in CLM4.5_old to 0.14 and –3.28 gC/m²/day in CLM4.5_new at BE-Vie and US-MMS, respectively. Estimated GPP from the start of carbon uptake duration to the date of carbon uptake amplitude at BE-Vie and US-MMS increased by 24.67% and 26.77%, respectively, for CLM4.5_new than for CLM4.5_old. The improvement in both carbon uptake duration and carbon uptake amplitude caused a total reduction in GPP bias at BE-Vie, US-PFa, and US-MMS, respectively.

3.4. Prediction of Phenology in China's Deciduous Forests in the Future

CLM4.5_new suggested a larger extension of growing season length (0.22 days/year) in 2016–2100, because of a greater advance rate in leaf unfolding dates (–0.11 days/year) and a delay in leaf falling dates (0.11 days/year) as shown in Figures 8a–8c. Most areas (95.11%) of China's deciduous forests experienced a substantial advance in leaf unfolding dates (Figure 8a), particularly in the subtropical region, where the temporal trend

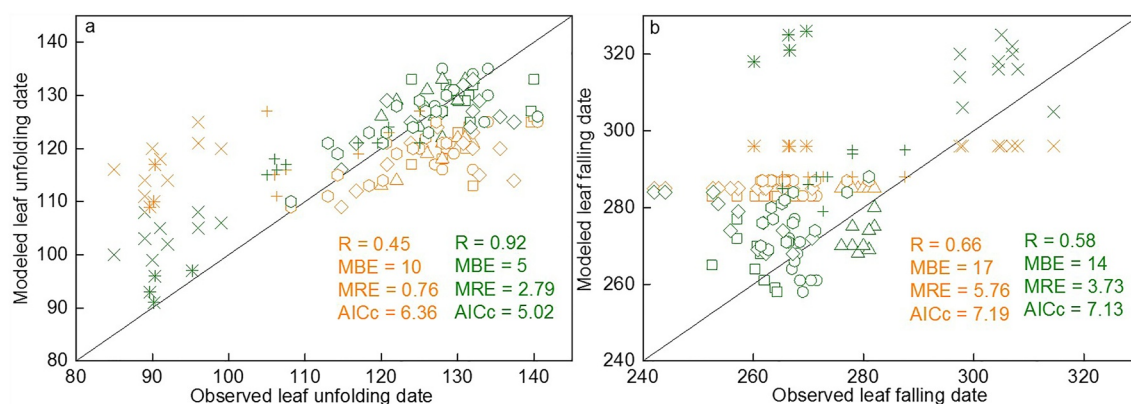


Figure 4. Evaluation of modeled leaf unfolding dates and leaf falling dates at eight sites of Chinese Phenological Observation Network (CPON). Orange: original CLM4.5 model, Green: modified CLM4.5 model. Square: Nenjiang (NJ), Circle: Dedu (DD), Triangle: Jiamusi (JMS), Diamond: Haerbin (HEB), Hexagon: Changchun (CC), Cross (+): Shenyang (SY), Cross (x): Luoyang (LY), Star: Xian (XA).

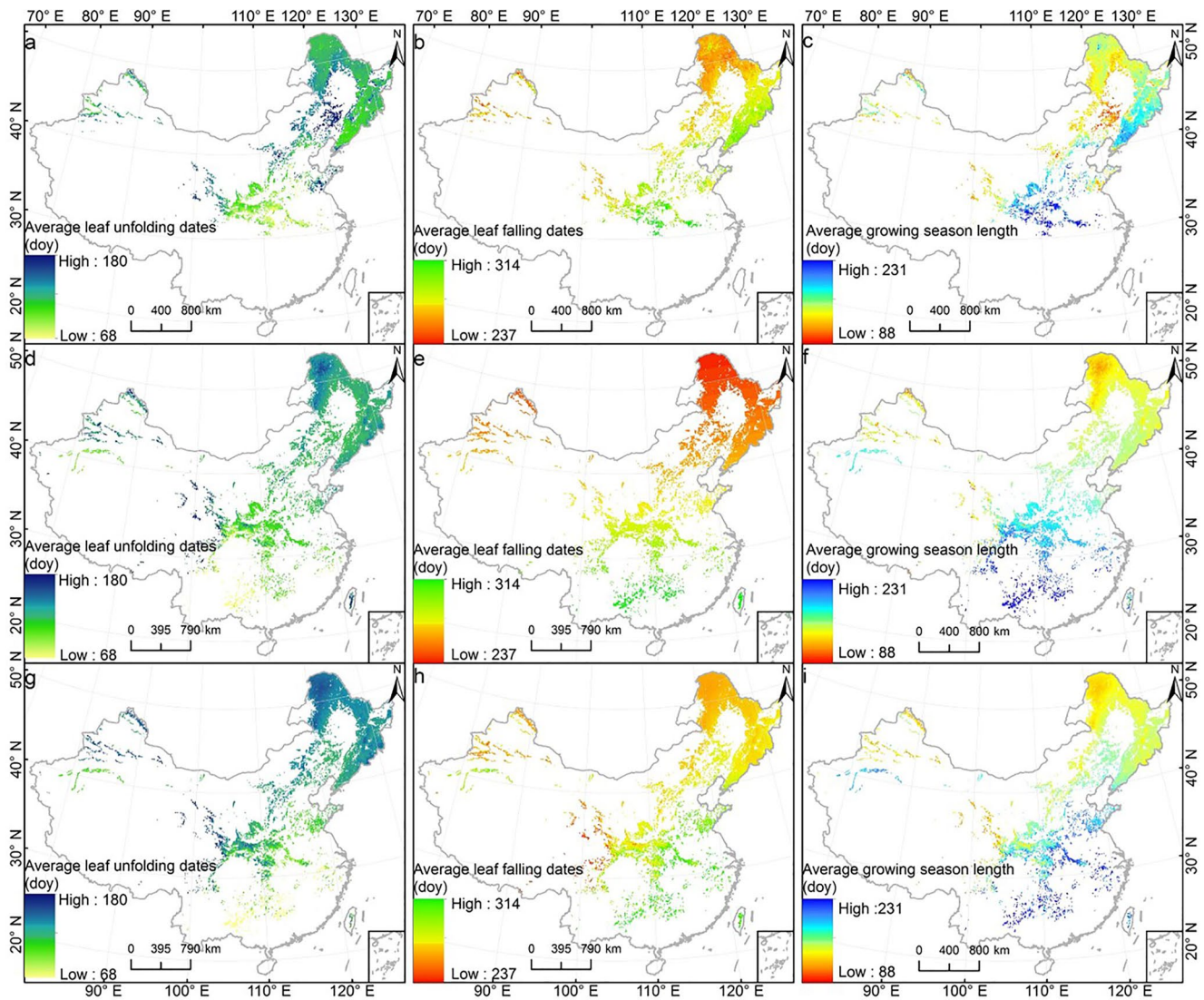


Figure 5. Spatial patterns of leaf unfolding dates, leaf falling dates, and growing season length in China's deciduous forests during 1982–2014. (a, b, c) spatial patterns of leaf unfolding dates, leaf falling dates, and growing season length derived from GIMMS NDVI3g. (d, e, f) spatial patterns of leaf unfolding dates, leaf falling dates, and growing season length modeled by the original CLM4.5 model. (g, h, i) spatial patterns of leaf unfolding dates, leaf falling dates, and growing season length modeled by the modified CLM4.5 model.

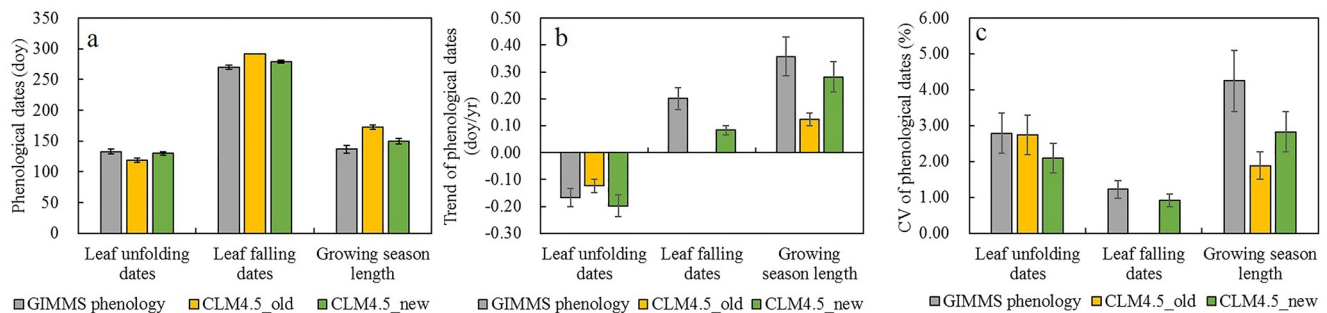


Figure 6. Comparisons of CLM4.5 modeled mean (a), trend (b), and coefficient of variation (c) of leaf unfolding dates, leaf falling dates, and growing season length with GIMMS phenology data over the period 1982–2014. The error bars represent one standard deviation.

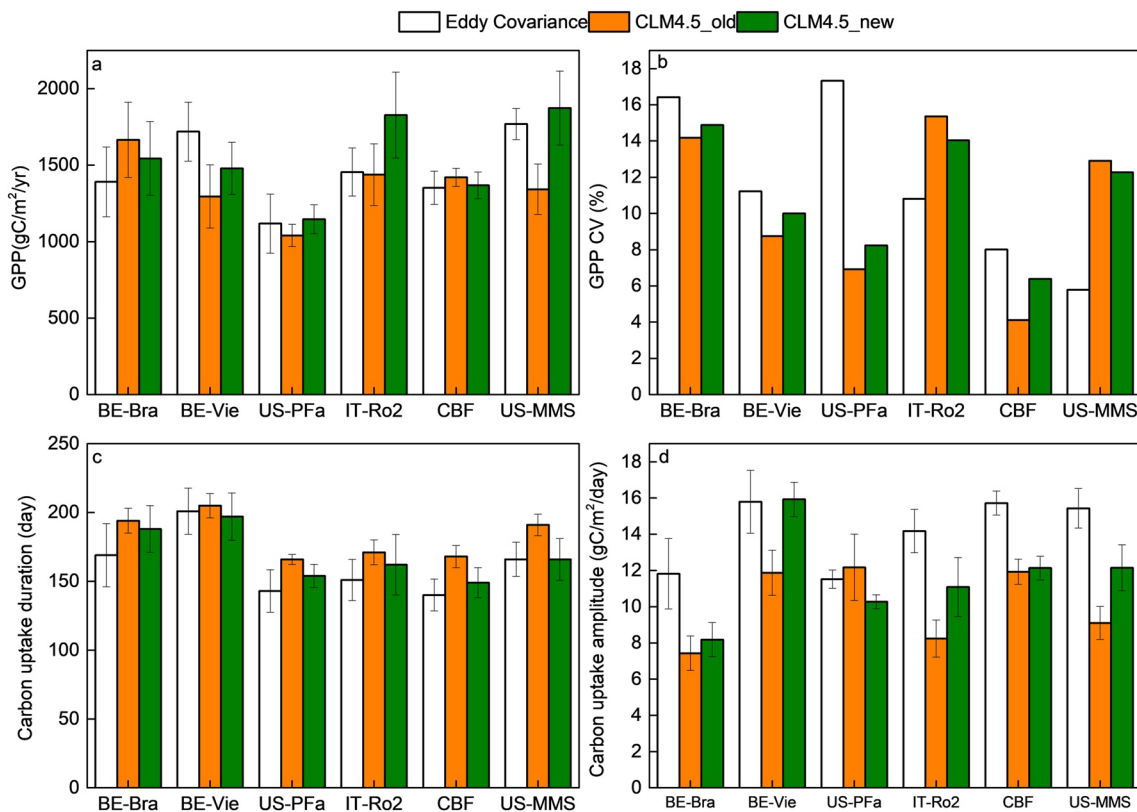


Figure 7. Comparison of annual Gross Primary Productivity (GPP) (a), interannual variation of GPP (b), carbon uptake duration (c), and carbon uptake amplitude (d) between original CLM4.5 (referred as to CLM4.5_old) and modified CLM4.5 (referred as to CLM4.5_new) at a forest site (CBF) of Chinese Ecosystem Research Network (CERN) and five forest sites of FLUXNET. The error bars in panels (a), (c), and (d) represent one standard deviation.

of leaf unfolding dates was -0.31 days/year (Figure 8g) with the highest increasing rate of mean pre-season temperature ($0.046^{\circ}\text{C}/\text{year}$, Figure S2e in Supporting Information S1). For the leaf falling dates, it delayed in most of China's deciduous forests (81.16%) because of remarkable temperature rise ($0.037^{\circ}\text{C}/\text{year}$, Figure S2f in Supporting Information S1), especially in the temperate region with significant increasing trend of 0.16 days/year (Figure 8h).

In contrast with the present, CLM4.5_new found the weaker advancement of leaf unfolding dates and the similar dependent of leaf falling dates under the RCP4.5 scenario in China's deciduous forests (Figures 8a, 8b, and 8d). With the trends of mean pre-season temperature decreased from $0.028^{\circ}\text{C}/\text{year}$ during 1981–2015 to $0.023^{\circ}\text{C}/\text{year}$ during 2016–2100 in RCP4.5 (Figures S2a and S2d in Supporting Information S1), the decrease of chill accumulation and the increase of heat requirement slowed down, while the former changed more, of which trends were reduced from -0.21 in 1981–2015 to -0.091 in 2016–2100 (Figures S3a and S3c in Supporting Information S1). To a certain extent, the reduction of chill accumulation increased the threshold of heat requirement and weakened the advance of leaf unfolding dates caused by climate warming. Although the delayed trend in leaf falling dates during 2016–2100 was similar to that during 1981–2015, but there was difference in three climatic regions. The delayed trend in leaf falling dates in the subtropical and temperate regions would reduce from 0.23 days/year and 0.10 days/year in 1981–2015 to 0.11 days/year and 0.11 days/year in 2016–2100 with the slowdown of warming in the future under the RCP4.5 scenario (Figure 8h, Figures S2b and S2d in Supporting Information S1). Moreover, the increasing rate in leaf falling dates in the cold temperate region was more substantial in 2016–2100 than in 1981–2015 (Figure 8h). The leaf unfolding and leaf falling dates in the last decade of the twenty-first century would be 8 days ahead of the current decade and 16 days later than the current decade modeled by CLM4.5_new, which lead to the 21 days extension of the growing season length. The difference in leaf falling dates' trend caused the difference in growing season length's trend over the periods 1981–2015 and 2016–2100. Consequently, the changing rates of growing season length from CLM4.5_new in the subtropical and temperate regions were only

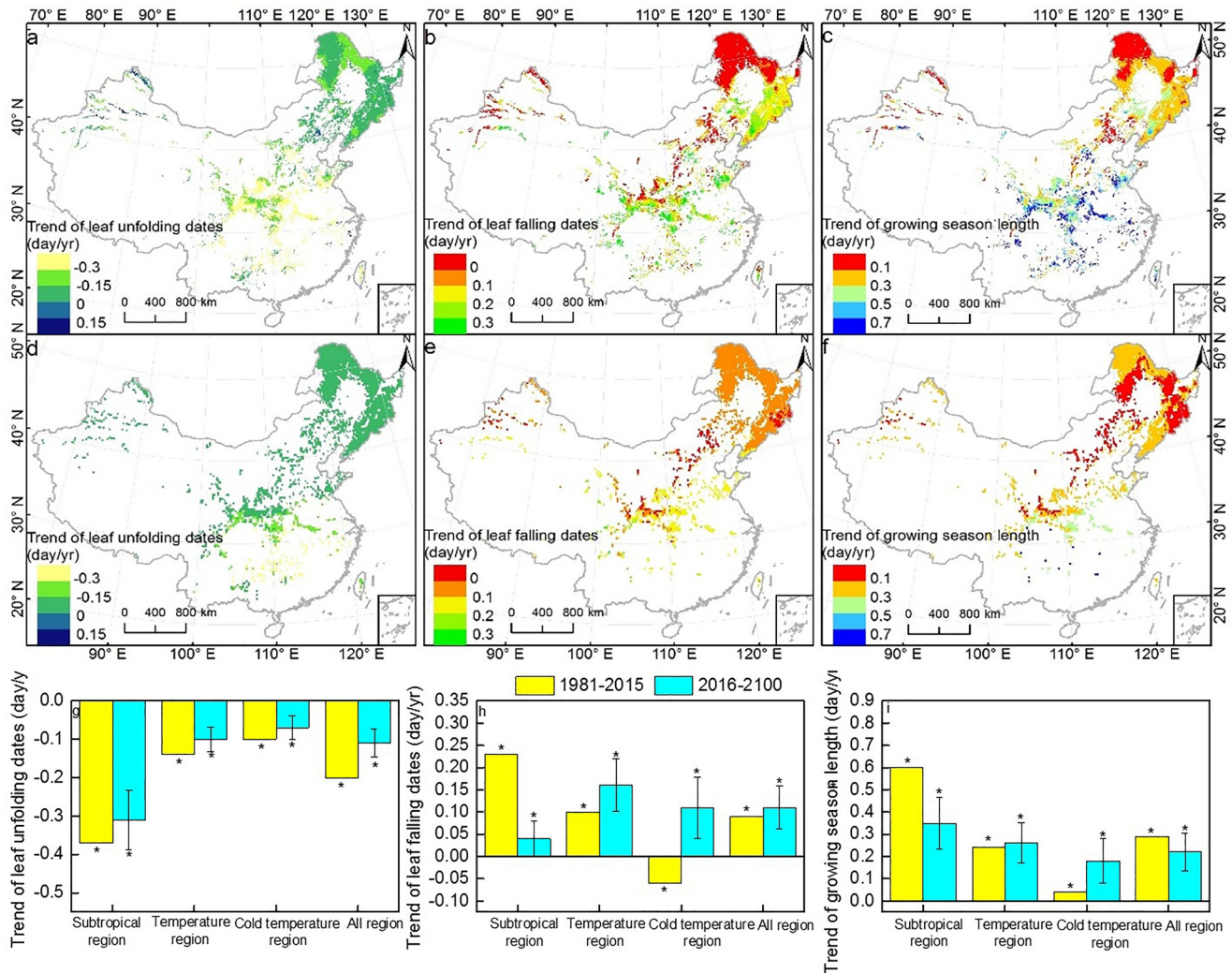


Figure 8. Trend of leaf unfolding dates (a, d, g), leaf falling dates (b, e, h), and growing season length (c, f, i) in China's deciduous forests during 1981–2015 (a, b, c) and 2016–2100 (d, e, f) under the RCP4.5 scenario modeled by modified CLM4.5. The error bars represent one standard deviation. * means $P < 0.05$, which is obtained by the statistical test using ANOVA.

about half of the current stage (Figure 8i). But the cold temperate region had a greater increasing trend in growing season length than that in 1981–2015 (Figure 8i).

The IAV was defined as detrended anomaly phenological dates in China's deciduous forests simulated by modified phenological models. The IAV in growing season length varied from -10.0 to 10.7 days during 2016–2100 under the RCP4.5 scenario in China's deciduous forests due to the IAV in leaf unfolding dates and leaf falling dates varying from -7.5 to 6.8 days and -6.2 to 6.8 days, respectively (Figures 9d–9f, Table S5 in Supporting Information S1). When compared with the other climatic regions, the subtropical region had a larger IAV in leaf unfolding dates (Table S5 in Supporting Information S1) because of the higher sensitivity of leaf unfolding dates to mean pre-season temperature (-0.71 days/ $^{\circ}\text{C}$, Table S6 in Supporting Information S1). The cold temperature region had a large IAV in leaf falling dates due to the large IAV of mean temperature before leaf falling dates (Table S5 in Supporting Information S1).

Compared with the current period, the IAV in phenological dates was similar in magnitude during 2016–2100 under the RCP4.5 scenario in China's deciduous forests on average (Table S5 in Supporting Information S1). Nevertheless, the IAV in phenological dates varied in different regions. The IAV of leaf unfolding dates in the subtropical and cold temperate regions during 2016–2100 more than doubled in comparison to the period of 1981–2015 due to the enhanced pre-season temperature IAV (Figure S4 and Table S5 in Supporting Information S1).

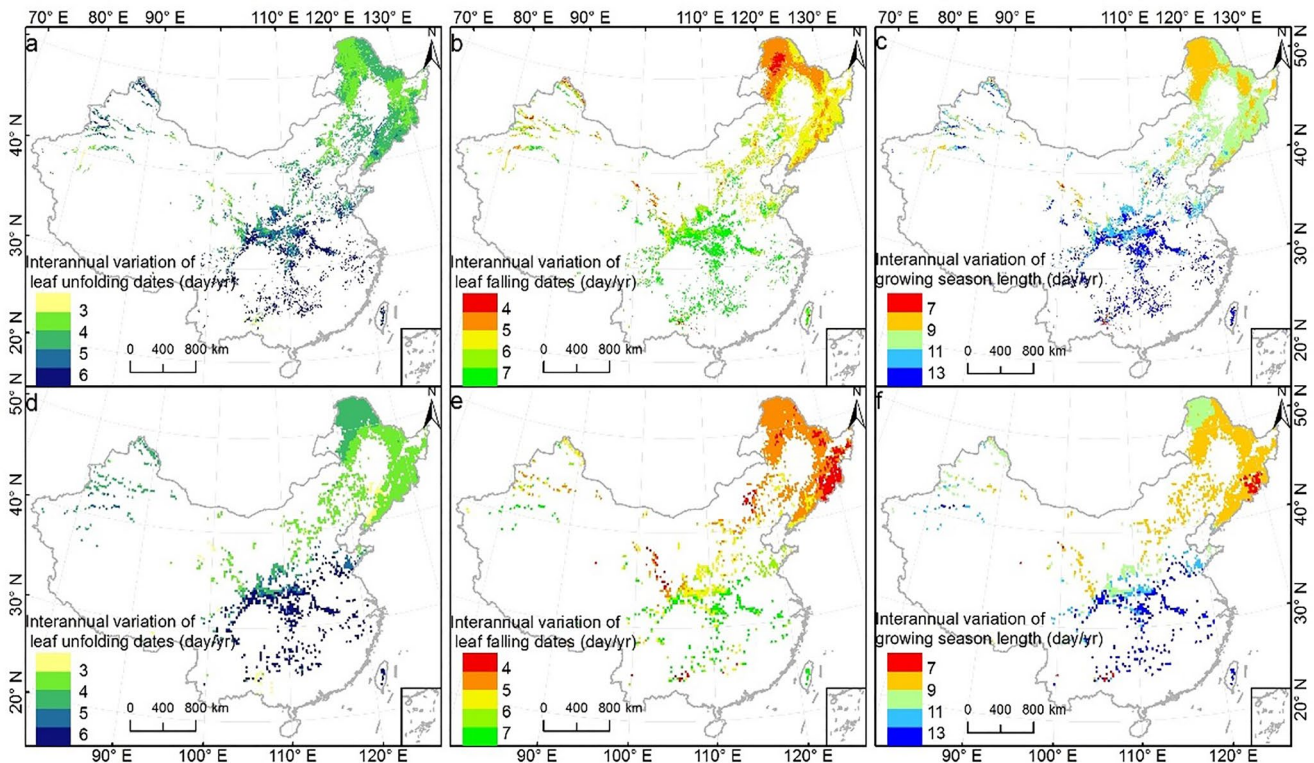


Figure 9. Interannual variations of leaf unfolding dates, leaf falling dates, and growing season length in China's deciduous forests during 1981–2015 (a, b, c) and during 2016–2100 under the RCP4.5 scenario (d, e, f) modeled by modified CLM4.5.

Further, the increase in IAV of heat requirement and chill accumulation led to strengthening IAV of leaf unfolding dates in the subtropical region (Figure S5 and Table S5 in Supporting Information S1). However, the enhanced IAV of leaf unfolding dates in the cold temperature region was mainly caused by the marked increase in IAV of heat requirement (from -45.82 and 35.95°C to -109.45 and 125.04°C) rather than a slight increase in chill accumulation (from -6.82 and 7.11°C to -9.04 and 11.44°C). In addition, the IAV of leaf falling dates in the cold temperate region increased by 50%, which was mainly caused by the enhanced preseason temperature IAV (Figure S4 in Supporting Information S1). In contrast, the decrease of cold-degree day summation induced the reduction in IAV of leaf falling dates in the subtropical and temperate regions (Figure S5 and Table S5 in Supporting Information S1). These results showed an increase in the IAV in growing season length driven by the increase in the IAV of preseason temperature, especially in the cold temperature region.

4. Discussion

Our results highlight the importance of modification on deciduous phenology simulation methods, especially the leaf-falling date, used in the CLM and most terrestrial biosphere models. Specifically, the low temperature threshold used in many models simulates the leaf falling with a high correlation but with a large deviation, and the daylength threshold method in CLM4.5 cannot reproduce the IAV of leaf falling dates and have remarkable bias (Table 6). The CDD/P model showed very good agreement with mean annual dates of leaf falling dates in France (Delpierre et al., 2009) and northern Minnesota of the U.S.A. (Meng et al., 2021), but it shows a large bias of leaf falling dates in this study (Table 6). Besides of low temperature and daylength, our study considered the effect of summer temperature on leaf falling (Lu and Keenan, 2022) in the new SummerIA model, which reduced the bias and RMSE of simulated leaf falling dates at the five CERN forest sites and was well consistent with remote sensed phenology at the national scale. Considering the two clusters of data in Figure 3, we removed the cold site (i.e., GGF) to examine the robust of the relationship between the average temperature from June to August and the aging state. The result show that exclusion of the data at GGF did not change this negative relationship and would not influence the simulation of leaf falling dates at these CERN sites (Table S1 in Supporting

Information S1). Moreover, the consideration of pre-season precipitation as documented in Liu et al. (2016) might improve the new model performance at MXF and SNF sites. Based on the relationship between precipitation in summer and the residual of observed and fitted aging state across four CERN forest sites (Figure S6 in Supporting Information S1), we expressed the threshold of the aging state at MXF and SNF sites as a function of precipitation sum from June to August. This update reduced the differences between observed and simulated leaf falling dates at MXF and SNF by 9 and 11 days, respectively. Underlying mechanisms of plant physiological processes (Bonan, 2015; Gepstein and Thimann, 1980) related to plant hormones and signal transduction (e.g., abscisic acid), and the role of source-sink feedbacks (Zani et al., 2020) are necessary to be considered in models in the future.

Whether the two-phase leaf unfolding models outperform the spring warming model remains controversial (Piao et al., 2019). Our results suggest that the alternating and parallel models had better performance in simulating leaf unfolding dates than using an individual heat requirement, as reported in previous studies (Harrington and Gould, 2015; Martínez-Lüscher et al., 2017). In addition, the performance of both alternating and parallel models depends on the expression of chill accumulation that largely affects the relationship between chill accumulation and the threshold of heat requirement (Figure 2). The variation in expression of chill accumulation results from different assumptions about the effectiveness of various temperatures for dormancy release (Harrington et al., 2010). Some studies have suggested that calculating the number of hours or days with temperatures less than 5°C were more effective than the other cold temperature thresholds (Cannell & Smith, 1983; Y. H. Fu et al., 2015). Models with a negative correlation based on CU1 gave a better result than those with a positive correlation based on CU2 or CU3. Experiments under a controlled environment indicated that additional chill accumulation before leaf unfolding dates may decrease the heat requirement (Couvillon and Erez, 1985; H. Wang et al., 2020). Therefore, the involvement of such a negative relationship between heat requirement and chill accumulation was regarded to be more reasonable and can improve model performance in simulating leaf unfolding dates (Chuine et al., 1999; Darbyshire et al., 2016; Y. H. Fu, Piao, et al., 2014; Y. H. Fu et al., 2015; B. Li et al., 2015). The alternating CU1 model remains a large deviation in some subtropical forests, possibly because those species have a small chilling requirement, which would lead to an earlier leaf unfolding date and might be at greater risk from early frost damage (Murray et al., 1989). It should be noted that the coefficients for calculating the threshold of leaf unfolding dates in different phenology models were fitted in our study. The model parameters may of course vary between species and locations. In a global change context, where the aim is the phenology modeling of populations, data concerning only some tree species would probably lead to deviated estimates (Chuine et al., 1998, 1999). Furthermore, more efforts on long-term species-specific phenology observations and digital photography monitoring for vegetation phenology (Melaas et al., 2016; Richardson et al., 2012) are also needed for evaluating and improving the model parameters and simulation of leaf phenology.

Introducing a new representation of the deciduous forests' phenology greatly improves the model's simulation of the variations of phenological dates and carbon cycles. Earlier spring leaf unfolding has been broadly observed but the amplitude of advancement varies with region and period (Piao et al., 2019). Using original and modified CLM4.5, our results all showed that deciduous trees in the subtropical region experienced the most significant trend of advanced leaf unfolding and delayed leaf falling when compared with those in the other two regions. This is consistent with the result from the phenological records in CPON that the greater advance in leaf unfolding dates in subtropical region than temperature region due to the higher sensitivity of leaf unfolding dates to spring temperature (H. Wang et al., 2015). Moreover, we found a weaker advancement of leaf unfolding dates during 2016–2100 under the RCP4.5 scenario in China's deciduous forests when compared with the period of 1981–2015. Since the leaf unfolding dates were affected by the tradeoff between heat requirement and chill accumulation (Gauzere et al., 2019), the advancement amplitude of leaf unfolding dates relies on both the change in threshold of heat requirement due to reduction of chill accumulation and the heat accumulation due to climate warming. Considering the chill accumulation, modified CLM4.5 made considerably more accurate leaf unfolding date predictions than the original CLM4.5. By contrast, the predicted delayed trend in leaf falling dates during 2016–2100 was similar to that during 1981–2015, except for the earlier leaf fall in the cold temperature region. This positive correlation between leaf falling dates and leaf unfolding dates has also been found in some records on the Qinghai—Tibetan Plateau (Lang et al., 2019), Europe (Y. H. Fu, Zhang, et al., 2014; Zani et al., 2020), and eastern United States (T. F. Keenan and Richardson, 2015). It is essential to consider such a relationship between leaf unfolding dates and leaf falling dates in earth system models.

Early spring phenology usually makes an increase in carbon uptake. For example, in the Northern Hemisphere, 1 day ahead of leaf unfolding dates results in an increase in GPP of approximately 0.2–8.4 gC/m²/day (Falge et al., 2002; Jeong et al., 2012; T. F. Keenan et al., 2014; Richardson et al., 2009). However, the delay of leaf falling dates may enhance the respiration (Richardson et al., 2009). In addition, extending the growing season length can increase the exposure to frost, which will damage leaves and reduce photosynthesis capacity and growth (Liu et al., 2018). The potential effects of future climate warming on the land carbon sink due to the change in phenology for deciduous forests in China needs further investigation.

More attention needs to be paid to the IAV of phenological dates, which is one of the important reasons for the uncertainty of the IAV of terrestrial carbon sink (T. F. Keenan et al., 2012a, 2012b). Compared with eddy covariance measurements, the ecosystem models underestimate the contribution of carbon uptake amplitude and overestimate the contribution of carbon uptake duration to the IAV of carbon sink, especially in forest ecosystems (Z. Fu et al., 2019). Our results suggest that the modification of phenology processes shows better behavior in predicting GPP and its IAV through improved estimation of both carbon uptake duration and carbon uptake amplitude (Figure 7 and Figure S1 in Supporting Information S1). The modified CLM4.5 outperforms the original CLM4.5 in terms of better accuracy of growing season length IAV due to the consideration of leaf falling dates IAV. In contrast with the current period, we found the enhanced IAV of leaf unfolding dates in subtropical region and the enhanced IAV of leaf falling dates in cold temperature region during 2016–2100 under the RCP4.5 scenario in China's deciduous forests due to the increased IAV of pre-season temperature. These results require further examination against long-term phenological observations in the subtropical and cold temperate regions of China.

5. Conclusions

We evaluated and modified the leaf unfolding and leaf falling models in deciduous trees using long-term phenological observations, and used the modified deciduous phenology models to quantify the changes in phenological dates and their regional differences. For the simulation of leaf unfolding dates, the parallel and alternating models performed better than the spring warming and sequential models, and their performance depends on the expression of chill accumulation. The new SummerIA model had better behavior in simulating the leaf falling dates than commonly-used models because of considering the relationship between summer temperature and aging state threshold. The modified phenology processes could improve the accuracy of the mean value and IAV of GPP because of the improvement of carbon uptake duration and amplitude. When compared with the original CLM4.5, modified CLM4.5 performs better in simulating spatial and temporal variations of phenological dates. The advance in leaf unfolding dates slowed down during 2016–2100 under the RCP4.5 scenario due to the reduction of climate warming compared to those during 1981–2015. By contrast, the delayed trend in leaf falling dates in the subtropical and temperate regions was reduced, while the trend in leaf falling dates in the cold temperate region switched from advance to delay. The subtropical region had a larger IAV in the leaf unfolding dates than the other two regions because of the highest sensitivity of phenological dates to pre-season temperature. The IAV of leaf unfolding dates and leaf falling dates in the cold temperate region increased due to the enhanced pre-season temperature IAV, in spite of the similar IAV of phenological dates in China's deciduous forests during the two periods. Our results highlight the urgency of modification of deciduous phenology simulation methods in CLM and the vital role of long-term phenology observations and mechanisms about the effects of plant hormones and signal transduction on leaf phenology for further improving phenology models.

Data Availability Statement

Long-term observed phenological data (CERN, 2020; Song et al., 2017) and hourly air temperature data (ChinaFLUX, 2021b) at five sites in Chinese Ecosystem Research Network (CERN) can be found in the Chinese Ecosystem Science Data Center. The phenological observations at eight sites in Chinese Phenological Observation Network (CPON) can be downloaded from the National Earth System Science Data Sharing Platform (Ge et al., 2014, 2015; H. Wang et al., 2014, 2015). Air temperature data at eight CPON sites were collected from the neighboring meteorological stations of China Meteorological Administration (2023). The ChinaFLUX data set is available at ChinaFlux (2021a). The FLUXNET data set is available at Pastorello et al., 2020. The temperature data from 1981 to 2015 were collected from the China Meteorological Forcing Data set (He et al., 2020). The daily temperature data in the RCP4.5 scenario were obtained from the NEX Global Daily Downscaled Climate

Projections (Thrasher et al., 2022). GIMMS Phenology data set was downloaded from X. Wang et al. (2019). Relevant data and code can be found at <https://figshare.com/s/741e0fb058fb81b6f07d>.

Acknowledgments

This work was supported by the National Natural Science Foundation of China (31971512, 31988102, 42141005). The authors appreciate the field staff from the stations of China Meteorological Administration, Chinese Ecosystem Research Network (Changbaishan, Beijing, Maoxian, Shenongjia, and Gonggashan Station), and ChinaFLUX (Changbaishan Station) for their contributions in long-term observation. We acknowledge the data support from “Chinese Ecosystem Science Data Center, National Science & Technology Infrastructure of China (<http://www.cnern.org.cn/>).” We acknowledge the data support from “National Earth System Science Data Sharing Infrastructure, National Science & Technology Infrastructure of China (<http://www.geodata.cn/>).” Flux data and climate data were from the FLUXNET2015 Data set, which includes data collected at BE-Bra, BE-Vie, US-PFa, IT-Ro2, and US-MMS stations from multiple regional flux networks. Climate scenarios in the future used were from the Global Daily Downscaled Projections (NEX-GDDP-CMIP6), prepared by the Climate Analytics Group and NASA Ames Research Center using the NASA Earth Exchange, and distributed by the NASA Center for Climate Simulation (NCCS). The authors are also grateful to the editors and anonymous reviewers.

References

- Abu-Asab, M. S., Peterson, P. M., Shetler, S. G., & Orli, S. S. (2001). Earlier plant flowering in spring as a response to global warming in the Washington, DC, area. *Biodiversity & Conservation*, 10(4), 597–612. <https://doi.org/10.1023/a:1016667125469>
- Archetti, M., Richardson, A. D., O’Keefe, J., & Delpierre, N. (2013). Predicting climate change impacts on the amount and duration of autumn colors in a New England forest. *PLoS One*, 8(3), e57373. <https://doi.org/10.1371/journal.pone.0057373>
- Basler, D., & Koerner, C. (2012). Photoperiod sensitivity of bud burst in 14 temperate forest tree species. *Agricultural and Forest Meteorology*, 165, 73–81. <https://doi.org/10.1016/j.agrformet.2012.06.001>
- Bonan, G. (2015). *Ecological climatology: Concepts and applications*. Cambridge University Press.
- Bradley, N. L., Leopold, A. C., Ross, J., & Huffaker, W. (1999). Phenological changes reflect climate change in Wisconsin. *Proceedings of the National Academy of Sciences of the United States of America*, 96(17), 9701–9704. <https://doi.org/10.1073/pnas.96.17.9701>
- Burnham, K., & Anderson, D. (2002). *Model selection and multimodel inference: A practical information-theoretic approach* (2nd ed.). Springer.
- Cannell, M. G. R., & Smith, R. I. (1983). Thermal time, chill days and prediction of budburst in *Picea sitchensis*. *Journal of Applied Ecology*, 20(3), 951–963. <https://doi.org/10.2307/2403139>
- Chen, M., Melaas, E. K., Gray, J. M., Friedl, M. A., & Richardson, A. D. (2016). A new seasonal-deciduous spring phenology submodel in the Community Land Model 4.5: Impacts on carbon and water cycling under future climate scenarios. *Global Change Biology*, 22(11), 3675–3688. <https://doi.org/10.1111/gcb.13326>
- ChinaFLUX. (2021a). 30 minute flux data of Changbaishan station from 2003 to 2010 [Dataset]. Chinese Ecosystem Science Data Center. <https://doi.org/10.12199/nescd.ecodb.chinaflux2003-2010.2020.cbf.005>
- ChinaFLUX. (2021b). 30 minute meteorological data of Changbaishan station from 2003 to 2010 [Dataset]. Chinese Ecosystem Science Data Center. <https://doi.org/10.12199/nescd.ecodb.chinaflux2003-2010.2020.cbf.001>
- China Meteorological Administration. (2023). Air temperature data at eight CPON sites (i.e., Nenjiang, Dedu, Jiamusi, Haerbin, Changchun, Shenyang, Luoyang and Xian) during 1986 – 2014 [Dataset]. Retrieved from <http://data.cma.cn>
- Chinese Ecosystem Research Network. (2020). Plant phenological observation dataset of the Chinese Ecosystem Research Network (2003-2015) [Dataset]. Science Data Bank. <https://doi.org/10.11922/sciencedb.318>
- Chuine, I., Cortazar-Atauri, I. G. D., Kramer, K., & Hänninen, H. (2013). *Plant development models, Phenology: An integrative environmental science* (pp. 275–293). Springer.
- Chuine, I., Cour, P., & Rousseau, D. (1998). Fitting models predicting dates of flowering of temperate-zone trees using simulated annealing. *Plant, Cell and Environment*, 21(5), 455–466. <https://doi.org/10.1046/j.1365-3040.1998.00299.x>
- Chuine, I., Cour, P., & Rousseau, D. (1999). Selecting models to predict the timing of flowering of temperate trees: Implications for tree phenology modelling. *Plant, Cell and Environment*, 22(1), 1–13. <https://doi.org/10.1046/j.1365-3040.1999.00395.x>
- Chuine, I., Morin, X., & Bugmann, H. (2010). Warming, photoperiods, and tree phenology. *Science*, 329(5989), 277–278. <https://doi.org/10.1126/science.329.5989.277-e>
- Churkina, G., Schimel, D., Braswell, B. H., & Xiao, X. M. (2005). Spatial analysis of growing season length control over net ecosystem exchange. *Global Change Biology*, 11(10), 1777–1787. <https://doi.org/10.1111/j.1365-2486.2005.00102.x>
- Cong, N., Wang, T., Nan, H., Ma, Y., Wang, X., Myneni, R., & Piao, S. (2013). Changes in satellite-derived spring vegetation green-up date and its linkage to climate in China from 1982 to 2010: A multimethod analysis. *Global Change Biology*, 19(3), 881–891. <https://doi.org/10.1111/gcb.12077>
- Couvillon, G., & Erez, A. (1985). Effect of level and duration of high temperatures on rest in the peach. *Journal of the American Society for Horticultural Science*, 110(4), 579–581. <https://doi.org/10.1094/Phyto-78-1352>
- Darbyshire, R., Pope, K., & Goodwin, I. (2016). An evaluation of the chill overlap model to predict flowering time in apple tree. *Scientia Horticulturae*, 198, 142–149. <https://doi.org/10.1016/j.scienta.2015.11.032>
- Delpierre, N., Dufrene, E., Soudani, K., Ulrich, E., Cechini, S., Boe, J., & Francois, C. (2009). Modelling interannual and spatial variability of leaf senescence for three deciduous tree species in France. *Agricultural and Forest Meteorology*, 149(6–7), 938–948. <https://doi.org/10.1016/j.agrformet.2008.11.014>
- El Masri, B., Shu, S., & Jain, A. K. (2015). Implementation of a dynamic rooting depth and phenology into a land surface model: Evaluation of carbon, water, and energy fluxes in the high latitude ecosystems. *Agricultural and Forest Meteorology*, 211, 85–99. <https://doi.org/10.1016/j.agrformet.2015.06.002>
- Estiarte, M., & Peñuelas, J. (2015). Alteration of the phenology of leaf senescence and fall in winter deciduous species by climate change: Effects on nutrient proficiency. *Global Change Biology*, 21(3), 1005–1017. <https://doi.org/10.1111/gcb.12804>
- Estrella, N., & Menzel, A. (2006). Responses of leaf colouring in four deciduous tree species to climate and weather in Germany. *Climate Research*, 32(3), 253–267. <https://doi.org/10.3354/cr032253>
- Falge, E., Baldocchi, D., Tenhunen, J., Aubinet, M., Bakwin, P., Berbigier, P., et al. (2002). Seasonality of ecosystem respiration and gross primary production as derived from FLUXNET measurements. *Agricultural and Forest Meteorology*, 113(1–4), 53–74. [https://doi.org/10.1016/S0168-1923\(02\)00102-8](https://doi.org/10.1016/S0168-1923(02)00102-8)
- Foley, J., Prentice, I., Ramankutty, N., Levis, S., Pollard, D., Sitch, S., & Haxeltine, A. (1996). An integrated biosphere model of land surface processes, terrestrial carbon balance, and vegetation dynamics. *Global Biogeochemical Cycles*, 10(4), 603–628. <https://doi.org/10.1029/96GB02692>
- Fu, Y. H., Campioli, M., Vitasse, Y., De Boeck, H. J., Van den Berge, J., AbdElgawad, H., et al. (2014). Variation in leaf flushing date influences autumnal senescence and next year’s flushing date in two temperate tree species. *Proceedings of the National Academy of Sciences of the United States of America*, 111(20), 7355–7360. <https://doi.org/10.1073/pnas.1321727111>
- Fu, Y. H., Li, X., Chen, S., Wu, Z., Su, J., Li, X., et al. (2022). Soil moisture regulates warming responses of autumn photosynthetic transition dates in subtropical forests. *Global Change Biology*, 28(16), 4935–4946. <https://doi.org/10.1111/gcb.16227>
- Fu, Y. H., Piao, S., de Beeck, M., Cong, N., Zhao, H., Zhang, Y., et al. (2014). Recent spring phenology shifts in western Central Europe based on multiscale observations. *Global Ecology and Biogeography*, 23(11), 1255–1263. <https://doi.org/10.1111/gcb.12210>
- Fu, Y. H., Zhang, H., Dong, W., & Yuan, W. (2014). Comparison of phenology models for predicting the onset of growing season over the Northern Hemisphere. *PLoS One*, 9(10), e109544. <https://doi.org/10.1371/journal.pone.0109544>

- Fu, Y. H., Zhao, H., Piao, S., Peaucelle, M., Peng, S., Zhou, G., et al. (2015). Declining global warming effects on the phenology of spring leaf unfolding. *Nature*, *526*(7571), 104–107. <https://doi.org/10.1038/nature15402>
- Fu, Z., Stoy, P., Luo, Y., Chen, J., Sun, J., Montagnani, L., et al. (2017). Climate controls over the net carbon uptake period and amplitude of net ecosystem production in temperate and boreal ecosystems. *Agricultural and Forest Meteorology*, *243*, 9–18. <https://doi.org/10.1016/j.agrformet.2017.05.009>
- Fu, Z., Stoy, P., Poulter, B., Gerken, T., Zhang, Z., Wakbulcho, G., & Niu, S. (2019). Maximum carbon uptake rate dominates the interannual variability of global net ecosystem exchange. *Global Change Biology*, *25*(10), 3381–3394. <https://doi.org/10.1111/gcb.14731>
- Gao, C., Zhang, Z., Chen, S., & Liu, Q. (2014). The high-resolution simulation of climate change model under RCP4.5 scenarios in the Huaihe River Basin. *Environmental Science Geographical Research*, *33*(3), 467–477. <https://doi.org/10.11821/dlyj201403006>
- Gauzere, J., Lucas, C., Ronce, O., Davi, H., & Chuine, I. (2019). Sensitivity analysis of tree phenology models reveals increasing sensitivity of their predictions to winter chilling temperature and photoperiod with warming climate. *Ecological Modelling*, *411*, 108805. <https://doi.org/10.1016/j.ecolmodel.2019.108805>
- Ge, Q., Wang, H., Rutishauser, T., & Dai, J. (2015). Phenological response to climate change in China: A meta-analysis. *Global Change Biology*, *21*(1), 265–274. <https://doi.org/10.1111/gcb.12648>
- Ge, Q., Wang, H., Zheng, J., Rutishauser, T., & Dai, J. (2014). A 170 year spring phenology index of plants in eastern China. *Journal of Geophysical Research: Biogeosciences*, *119*(3), 301–310. <https://doi.org/10.1002/2013JG002565>
- Gepstein, S., & Thimann, K. V. (1980). Changes in the abscisic-acid content of oat leaves during senescence. *Proceedings of the National Academy of Sciences of the United States of America*, *77*(4), 2050–2053. <https://doi.org/10.1073/pnas.77.4.20>
- Ghelardini, L., Santini, A., Black-Samuelsson, S., Myking, T., & Falusi, M. (2010). Bud dormancy release in elm (*Ulmus* spp.) clones—a case study of photoperiod and temperature responses. *Tree Physiology*, *30*(2), 264–274. <https://doi.org/10.1093/treephys/tpp110>
- Gu, F. (2007). Mechanistic simulation of the key ecological processes of water and carbon cycles in typical terrestrial ecosystems and the comparisons with eddy flux measurements (Dissertation for Doctor of Philosophy). Graduate University of Chinese Academy of Sciences.
- Gu, L., Post, W., Baldocchi, D., Black, T., Suyker, A., Verma, S., et al. (2009). *Characterizing the seasonal dynamics of plant community photosynthesis across a range of vegetation types, Phenology of ecosystem processes* (pp. 35–58). Springer.
- Hänninen, H. (1990). Modelling bud dormancy release in trees from cool and temperate regions. *Acta Forestalia Fennica*, *213*(213), 47. <https://doi.org/10.14214/aff.7660>
- Hänninen, H. (1996). Effects of climatic warming on northern trees: Testing the frost damage hypothesis with meteorological data from provenance transfer experiments. *Scandinavian Journal of Forest Research*, *11*(1–4), 17–25. <https://doi.org/10.1080/02827589609382908>
- Harrington, C., & Gould, P. (2015). Tradeoffs between chilling and forcing in satisfying dormancy requirements for Pacific Northwest tree species. *Frontiers in Plant Science*, *6*, 120. <https://doi.org/10.3389/fpls.2015.00120>
- Harrington, C., Gould, P., & Clair, J. (2010). Modeling the effects of winter environment on dormancy release of Douglas-fir. *Forest Ecology and Management*, *259*(4), 798–808. <https://doi.org/10.1016/j.foreco.2009.06.018>
- He, J., Yang, K., Tang, W., Lu, H., Qin, J., Chen, Y., & Li, X. (2020). The first high-resolution meteorological forcing dataset for land process studies over China [Dataset]. *Scientific Data*, *7*(1), 25. <https://doi.org/10.1038/s41597-020-0369-y>
- Heide, O. (1993). Daylength and thermal time responses of budburst during dormancy release in some northern deciduous trees. *Physiologia Plantarum*, *88*(4), 531–540. <https://doi.org/10.1111/j.1399-3054.1993.tb01368.x>
- Horemans, J., Henrot, A., Delire, C., Kollas, C., Lasch-Born, P., Reyer, C., et al. (2017). Combining multiple statistical methods to evaluate the performance of process-based vegetation models across three forest stands. *Central European Forestry Journal*, *63*(4), 153–172. <https://doi.org/10.1515/forj-2017-0025>
- Huang, K., & Xia, J. (2019). High ecosystem stability of evergreen broadleaf forests under severe droughts. *Global Change Biology*, *25*(10), 3494–3503. <https://doi.org/10.1111/gcb.14748>
- Jeong, S.-J., Medvigy, D., Shevliakova, E., & Malyshev, S. (2012). Uncertainties in terrestrial carbon budgets related to spring phenology. *Journal of Geophysical Research*, *117*(G1), G01030. <https://doi.org/10.1029/2011JG001868>
- Jia, B., Wang, Y., & Xie, Z. (2018). Responses of the terrestrial carbon cycle to drought over China: Modeling sensitivities of the interactive nitrogen and dynamic vegetation. *Ecological Modelling*, *368*, 52–68. <https://doi.org/10.1016/j.ecolmodel.2017.11.009>
- Keenan, D. (2014). Statistical analyses of surface temperatures in the IPCC Fifth Assessment Report.
- Keenan, T. F., Baker, I., Barr, A., Ciais, P., Davis, K., Dietze, M., et al. (2012a). Terrestrial biosphere model performance for inter-annual variability of land-atmosphere CO₂ exchange. *Global Change Biology*, *18*(6), 1971–1987. <https://doi.org/10.1111/j.1365-2486.2012.02678.x>
- Keenan, T. F., Davidson, E. A., Moffat, A. M., Munger, W., & Richardson, A. D. (2012b). Using model-data fusion to interpret past trends, and quantify uncertainties in future projections, of terrestrial ecosystem carbon cycling. *Global Change Biology*, *18*(8), 2555–2569. <https://doi.org/10.1111/j.1365-2486.2012.02684.x>
- Keenan, T. F., Gray, J., Friedl, M., Toomey, M., Bohrer, G., Hollinger, D., et al. (2014). Net carbon uptake has increased through warming-induced changes in temperate forest phenology. *Nature Climate Change*, *4*(7), 598–604. <https://doi.org/10.1038/NCLIMATE2253>
- Keenan, T. F., & Richardson, A. D. (2015). The timing of autumn senescence is affected by the timing of spring phenology: Implications for predictive models. *Global Change Biology*, *21*(7), 2634–2641. <https://doi.org/10.1111/gcb.12890>
- Kramer, K. (1994). Selecting a model to predict the onset of growth of *Fagus sylvatica*. *Journal of Applied Ecology*, *31*(1), 172–181. <https://doi.org/10.1046/j.1365-3040.1999.00395.x>
- Kramer, K., Leinonen, I., & Loustau, D. (2000). The importance of phenology for the evaluation of impact of climate change on growth of boreal, temperate and Mediterranean forests ecosystems: An overview. *International Journal of Biometeorology*, *44*(2), 67–75. <https://doi.org/10.1007/s004840000066>
- Krinner, G., Viovy, N., de Noblet-Ducoudré, N., Ogée, J., Polcher, J., Friedlingstein, P., et al. (2005). A dynamic global vegetation model for studies of the coupled atmosphere-biosphere system. *Global Biogeochemical Cycles*, *19*(1), GB1015. <https://doi.org/10.1029/2003GB002199>
- Landsberg, J. (1974). Apple fruit bud development and growth; analysis and an empirical model. *Annals of Botany*, *38*(5), 1013–1023. <https://doi.org/10.1093/oxfordjournals.aob.a084891>
- Lang, W., Chen, X., Qian, S., Liu, G., & Piao, S. (2019). A new process-based model for predicting autumn phenology: How is leaf senescence controlled by photoperiod and temperature coupling? *Agricultural and Forest Meteorology*, *268*, 124–135. <https://doi.org/10.1016/j.agrformet.2019.01.006>
- Lawrence, D. M., Fisher, R. A., Koven, C. D., Oleson, K. W., Swenson, S. C., Bonan, G., et al. (2019). The Community Land Model version 5: Description of new features, benchmarking, and impact of forcing uncertainty. *Journal of Advances in Modeling Earth Systems*, *11*(12), 4245–4287. <https://doi.org/10.1029/2018MS001583>
- Lechowicz, M. (1984). Why do temperate deciduous trees leaf out at different times? Adaptation and ecology of forest communities. *The American Naturalist*, *124*(6), 821–842. <https://doi.org/10.1086/284319>

- Li, B., Guo, B., Li, H., & Shi, Y. (2015). An analytical solution to simulate the effect of cement/formation stiffness on well integrity evaluation in carbon sequestration projects. *Journal of Natural Gas Science and Engineering*, 27, 1092–1099. <https://doi.org/10.1016/j.jngse.2015.09.058>
- Li, P., Zhang, L., Yu, G., Liu, C., Ren, X., He, H., et al. (2018). Interactive effects of seasonal drought and nitrogen deposition on carbon fluxes in a subtropical evergreen coniferous forest in the East Asian monsoon region. *Agricultural and Forest Meteorology*, 263, 90–99. <https://doi.org/10.1016/j.agrformet.2018.08.009>
- Liu, Q., Fu, Y., Zhu, Z., Liu, Y., Liu, Z., Huang, M., et al. (2016). Delayed autumn phenology in the Northern Hemisphere is related to change in both climate and spring phenology. *Global Change Biology*, 22(11), 3702–3711. <https://doi.org/10.1111/gcb.13311>
- Liu, Q., Piao, S., Janssens, I. A., Fu, Y., Peng, S., Lian, X. U., et al. (2018). Extension of the growing season increases vegetation exposure to frost. *Nature Communications*, 9(1), 426. <https://doi.org/10.1038/s41467-017-02690-y>
- Lu, X., & Keenan, T. F. (2022). No evidence for a negative effect of growing season photosynthesis on leaf senescence timing. *Global Change Biology*, 28(9), 3083–3093. <https://doi.org/10.1111/gcb.16104>
- Lundell, R., Hänninen, H., Saarinen, T., Åström, H., & Zhang, R. (2020). Beyond rest and quiescence (endodormancy and ecodormancy): A novel model for quantifying plant–environment interaction in bud dormancy release. *Plant, Cell and Environment*, 43(1), 40–54. <https://doi.org/10.1111/pce.13650>
- Lv, Y., Zhang, L., Li, P., He, H., Ren, X., & Zhang, M. (2023). Ecological restoration projects enhanced terrestrial carbon sequestration in the karst region of Southwest China. *Frontiers in Ecology and Evolution*, 11, 312. <https://doi.org/10.3389/fevo.2023.1179608>
- MacBean, N., Maignan, F., Peylin, P., Bacour, C., Bréon, F., & Ciais, P. (2015). Using satellite data to improve the leaf phenology of a global terrestrial biosphere model. *Biogeosciences*, 12(23), 7185–7208. <https://doi.org/10.5194/bg-12-7185-2015>
- Martínez-Lüscher, J., Hadley, P., Ordidge, M., Xu, X., & Luedeling, E. (2017). Delayed chilling appears to counteract flowering advances of apricot in southern UK. *Agricultural and Forest Meteorology*, 237–238, 209–218. <https://doi.org/10.1016/j.agrformet.2017.02.017>
- Melaas, E., Friedl, M., & Richardson, A. (2016). Multiscale modeling of spring phenology across deciduous forests in the Eastern United States. *Global Change Biology*, 22(2), 792–805. <https://doi.org/10.1111/gcb.13122>
- Meng, L., Mao, J., Ricciuto, D., Shi, X., Richardson, A., Hanson, P., et al. (2021). Evaluation and modification of ELM seasonal deciduous phenology against observations in a southern boreal peatland forest. *Agricultural and Forest Meteorology*, 308–309, 108556. <https://doi.org/10.1016/j.agrformet.2021.108556>
- Menzel, A., Sparks, T. H., Estrella, N., & Roy, D. (2006). Altered geographic and temporal variability in phenology in response to climate change. *Global Ecology and Biogeography*, 15(5), 498–504. <https://doi.org/10.1111/j.1466-822X.2006.00247.x>
- Murray, M., Cannell, M., & Smith, R. (1989). Date of budburst of fifteen tree species in Britain following climatic warming. *Journal of Applied Ecology*, 26(2), 693–700. <https://doi.org/10.2307/2404093>
- Oleson, K., Lawrence, D., Bonan, G., Drewniak, B., Huang, M., Koven, C., et al. (2013). *Technical description of version 4.5 of the Community Land Model (CLM)*. NCAR Technical Note: NCAR/TN-503+ STR. National Center for Atmospheric Research (NCAR). <https://doi.org/10.5065/D6RR1W7MM>
- Pastorello, G., Trotta, C., Canfora, E., Christianson, D., Cheah, Y. W., Torn, M., et al. (2020). The FLUXNET2015 dataset and the ONEFlux processing pipeline for eddy covariance data. *Scientific Data*, 7(1), 225. <https://doi.org/10.1038/s41597-020-0534-3>
- Peaucelle, M., Janssens, I., Stocker, B., Ferrando, A., Fu, Y., Molowny-Horas, R., et al. (2019). Spatial variance of spring phenology in temperate deciduous forests is constrained by background climatic conditions. *Nature Communications*, 10(1), 5388. <https://doi.org/10.1038/s41467-019-13365-1>
- Piao, S., Friedlingstein, P., Ciais, P., Viovy, N., & Demarty, J. (2007). Growing season extension and its impact on terrestrial carbon cycle in the Northern Hemisphere over the past 2 decades. *Global Biogeochemical Cycles*, 21(3), GB3018. <https://doi.org/10.1029/2006GB002888>
- Piao, S., Liu, Q., Chen, A., Janssens, I., Fu, Y., Dai, J., et al. (2019). Plant phenology and global climate change: Current progresses and challenges. *Global Change Biology*, 25(6), 1922–1940. <https://doi.org/10.1111/gcb.14619>
- Piao, S., Sitch, S., Ciais, P., Friedlingstein, P., Peylin, P., Wang, X., et al. (2013). Evaluation of terrestrial carbon cycle models for their response to climate variability and to CO₂ trends. *Global Change Biology*, 19(7), 2117–2132. <https://doi.org/10.1111/gcb.12187>
- Piao, S., Tan, J., Chen, A., Fu, Y., Ciais, P., Liu, Q., et al. (2015). Leaf onset in the Northern Hemisphere triggered by daytime temperature. *Nature Communications*, 6(1), 6911. <https://doi.org/10.1038/ncomms7911>
- Richardson, A., Anderson, R., Arain, M., Barr, A., Bohrer, G., Chen, G., et al. (2012). Terrestrial biosphere models need better representation of vegetation phenology: Results from the North American Carbon Program Site Synthesis. *Global Change Biology*, 18(2), 566–584. <https://doi.org/10.1111/j.1365-2486.2011.02562.x>
- Richardson, A., Black, T., Ciais, P., Delbart, N., Friedl, M., Gobron, N., et al. (2010). Influence of spring and autumn phenological transitions on forest ecosystem productivity. *Philosophical Transactions of the Royal Society of London. Series B, Biological Sciences*, 365(1555), 3227–3246. <https://doi.org/10.1098/rstb.2010.0102>
- Richardson, A., Hollinger, D., Dail, D., Lee, J., Munger, J., & O'Keefe, J. (2009). Influence of spring phenology on seasonal and annual carbon balance in two contrasting New England forests. *Tree Physiology*, 29(3), 321–331. <https://doi.org/10.1093/treephys/tpn040>
- Sarvas, R. (1972). Investigations on the annual cycle of development of forest trees. Active period. *Communication Environmental Science*, 76(3), 1–110.
- Sarvas, R. (1974). Investigations on the annual cycle of development of forest trees. II. Autumn dormancy and winter dormancy. *Environmental Science*, 84(1), 1–101.
- Shiga, Y. P., Michalak, A. M., Fang, Y., Schaefer, K., Andrews, A. E., Huntzinger, D. H., et al. (2018). Forests dominate the interannual variability of the North American carbon sink. *Environmental Research Letters*, 13(8), 084015. <https://doi.org/10.1088/1748-9326/aad505>
- Sitch, S., Mitchell, B., Prentice, I., Arneth, A., Bondeau, A., Cramer, W., et al. (2003). Evaluation of ecosystem dynamics, plant geography and terrestrial carbon cycling in the LPJ dynamic global vegetation model. *Global Change Biology*, 9(2), 161–185. <https://doi.org/10.1046/j.1365-2486.2003.00569.x>
- Song, C., Zhang, L., Wu, D., Bai, F., Feng, J., Feng, L., et al. (2017). Plant phenological observation dataset of the Chinese Ecosystem Research Network (2003 – 2015) [Dataset]. China Scientific Data, 2(1), 27–34. <https://doi.org/10.11922/csdata.180.2016.0110>
- Thrasher, B., Wang, W., Michaelis, A., Melton, F., Lee, T., & Nemani, R. (2022). NASA global daily downscaled projections, CMIP6 [Dataset]. Scientific Data, 9(1), 262. <https://doi.org/10.1038/s41597-022-01393-4>
- Tian, H., Melillo, J., Lu, C., Kicklighter, D., Liu, M., Ren, W., et al. (2011). China's terrestrial carbon balance: Contributions from multiple global change factors. *Global Biogeochemical Cycles*, 25(1), GB1007. <https://doi.org/10.1029/2010GB003838>
- Verseghy, D., McFarlane, N., & Lazare, M. (1993). Class-A Canadian land surface scheme for GCMs. II. Vegetation model and coupled runs. *International Journal of Climatology*, 13(4), 347–370. <https://doi.org/10.1002/joc.3370130402>
- Vitasse, Y., François, C., Delpierre, N., Dufrene, E., Kremer, A., Chuine, I., & Delzon, S. (2011). Assessing the effects of climate change on the phenology of European temperate trees. *Agricultural and Forest Meteorology*, 151(7), 969–980. <https://doi.org/10.1016/j.agrformet.2011.03.003>

- Wang, H., Dai, J., Zheng, J., & Ge, Q. (2014). Temperature sensitivity of plant phenology in temperate and subtropical regions of China from 1850 to 2009. *International Journal of Climatology*, *35*(6), 913–922. <https://doi.org/10.1002/joc.4026>
- Wang, H., Ge, Q., Rutishauser, T., Dai, Y., & Dai, J. (2015). Parameterization of temperature sensitivity of spring phenology and its application in explaining diverse phenological responses to temperature change. *Scientific Reports*, *5*(1), 8833. <https://doi.org/10.1038/srep08833>
- Wang, H., Wu, C., Ciais, P., Peñuelas, J., Dai, J., Fu, Y., & Ge, Q. (2020). Overestimation of the effect of climatic warming on spring phenology due to misrepresentation of chilling. *Nature Communications*, *11*(1), 4945. <https://doi.org/10.1038/s41467-020-18743-8>
- Wang, M., Li, P., Peng, C., Xiao, J., Zhou, X., Luo, Y., & Zhang, C. (2022). Divergent responses of autumn vegetation phenology to climate extremes over northern middle and high latitudes. *Global Ecology and Biogeography*, *31*(11), 2281–2296. <https://doi.org/10.1111/geb.13583>
- Wang, X., Xiao, J., Li, X., Cheng, G., Ma, M., Che, T., et al. (2017). No consistent evidence for advancing or delaying trends in spring phenology on the Tibetan Plateau. *Journal of Geophysical Research: Biogeosciences*, *122*(12), 3288–3305. <https://doi.org/10.1002/2017JG003949>
- Wang, X., Xiao, J., Li, X., Cheng, G., Ma, M., Zhu, G., et al. (2019). No trends in spring and autumn phenology during the global warming hiatus. *Nature Communications*, *10*(1), 2389. <https://doi.org/10.1038/s41467-019-10235-8>
- Wareing, P. (1956). Photoperiodism in woody plants. *Annual Review of Plant Physiology*, *7*(1), 191–214. <https://doi.org/10.1146/annurev.pp.07.060156.001203>
- White, M., Thornton, P., & Running, S. (1997). A continental phenology model for monitoring vegetation responses to interannual climatic variability. *Global Biogeochemical Cycles*, *11*(2), 217–234. <https://doi.org/10.1029/97GB00330>
- Wu, B., Yuan, Q., Yan, C., Wang, Z., Yu, X., Li, A., et al. (2014). Land cover changes of China from 2000 to 2010. *Quaternary Sciences*, *34*(4), 723–731.
- Xia, J., Niu, S., Ciais, P., Janssens, I., Chen, J., Ammann, C., et al. (2015). Joint control of terrestrial gross primary productivity by plant phenology and physiology. *Proceedings of the National Academy of Sciences of the United States of America*, *112*(9), 2788–2793. <https://doi.org/10.1073/pnas.1413090112>
- Xue, W., Zhang, J., Ji, D., Che, Y., Lu, T., Deng, X., et al. (2021). Aerosol-induced direct radiative forcing effects on terrestrial ecosystem carbon fluxes over China. *Environmental Research*, *200*, 111464. <https://doi.org/10.1016/j.envres.2021.111464>
- Yang, X., Zhou, B., Xu, Y., & Han, Z. (2021). CMIP6 evaluation and projection of temperature and precipitation over China. *Advances in Atmospheric Sciences*, *38*(5), 817–830. <https://doi.org/10.1007/s00376-021-0351-4>
- Zani, D., Crowther, T. W., Mo, L., Renner, S. S., & Zohner, C. M. (2020). Increased growing-season productivity drives earlier autumn leaf senescence in temperate trees. *Science*, *370*(6520), 1066–1071. <https://doi.org/10.1126/science.abd8911>
- Zhang, L., Mao, J., Shi, X., Ricciuto, D., He, H., Thornton, P., et al. (2016). Evaluation of the Community Land Model simulated carbon and water fluxes against observations over ChinaFLUX sites. *Agricultural and Forest Meteorology*, *226*, 174–185. <https://doi.org/10.1016/j.agrformet.2016.05.018>
- Zhang, L., Ren, X., Wang, J., He, H., Wang, S., Wang, M., et al. (2019). Interannual variability of terrestrial net ecosystem productivity over China: Regional contributions and climate attribution. *Environmental Research Letters*, *14*(1), 014003. <https://doi.org/10.1088/1748-9326/aaec95>
- Zhao, M., Peng, C., Xiang, W., Deng, X., Tian, D., Zhou, X., et al. (2013). Plant phenological modeling and its application in global climate change research: Overview and future challenges. *Environmental Reviews*, *21*(1), 1–14. <https://doi.org/10.1139/er-2012-0036>